NAVAL POSTGRADUATE SCHOOL
Monterey, California

THESIS

COMPUTER SIMULATION OF COPPER IN THE
LIQUID PHASE AND THE SPUTTERING OF
LIQUID COPPER BY ONE KEV ARGON IONS

by

Raul de Jesus Rodriguez

December 1988

Thesis Advisor: Roger Smith

Approved for public release; distribution is unlimited

REPORT DOCUMENTATION PAGE

Report Security Classification Unclassified		1b Restrictive Markings			
Security Classification Authority		3 Distribution Availability of Report			
Declassification Downgrading Schedule		Approved for public release; distribution is unlimited.			
Performing Organization Report Number(s)		5 Monitoring Organization Report Number(s)			
Name of Performing Organization aval Postgraduate School	6b Office Symbol *(if applicable)* 61	7a Name of Monitoring Organization Naval Postgraduate School			
Address *(city, state, and ZIP code)* onterey, CA 93943-5000		7b Address *(city, state, and ZIP code)* Monterey, CA 93943-5000			
Name of Funding Sponsoring Organization	8b Office Symbol *(if applicable)*	9 Procurement Instrument Identification Number			
Address *(city, state, and ZIP code)*		10 Source of Funding Numbers			
		Program Element No	Project No	Task No	Work Unit Accession No

Title *(include security classification)* COMPUTER SIMULATION OF COPPER IN THE LIQUID PHASE AND THE PUTTERING OF LIQUID COPPER BY ONE KEV ARGON IONS.

Personal Author(s) Raul de Jesus Rodriguez

a Type of Report aster's Thesis	13b Time Covered From To	14 Date of Report *(year, month, day)* December 1988	15 Page Count 106

Supplementary Notation The views expressed in this thesis are those of the author and do not reflect the official policy or po-
ion of the Department of Defense or the U.S. Government.

Cosati Codes			18 Subject Terms *(continue on reverse if necessary and identify by block number)*
eld	Group	Subgroup	Liquid Copper, Computer Simulation, Sputtering.

Abstract *(continue on reverse if necessary and identify by block number)*
A molecular dynamics computer simulation was used to investigate several techniques of generating liquid Cu targets.
he target with the best liquid characteristics was subjected to one KeV, argon ion bombardment as a preliminary study of
e sputtering of liquids. The techniques of warming by impulse and warming by initially displacing atoms from their equi-
rium positions were compared. Both methods produced targets with good liquid properties. The energy became equally
rtitioned between kinetic and potential energy and all targets equilibrated within 400 fs. The range of a typical atom during
e time of equilibration was found to be restricted to its initial neighborhood. The preliminary sputtering study resulted in
sputtering yield increase of 40% over the solid target, for a low index crystal plane.

Distribution Availability of Abstract unclassified unlimited ☐ same as report ☐ DTIC users	21 Abstract Security Classification Unclassified	
a Name of Responsible Individual oger Smith	22b Telephone *(include Area code)* (408) 646-2697	22c Office Symbol 61Sm

FORM 1473,84 MAR   83 APR edition may be used until exhausted   security classification of this page
                         All other editions are obsolete

                                                                            Unclassified

Computer Simulation of Copper in the Liquid Phase
and the Sputtering of Liquid Copper by One KeV Argon Ions

by

Raul de Jesus Rodriguez
Lieutenant, United States Navy
B.S., University of Florida, 1981

Submitted in partial fulfillment of the
requirements for the degree of

MASTER OF SCIENCE IN PHYSICS

from the

NAVAL POSTGRADUATE SCHOOL
December 1988

ABSTRACT

A molecular dynamics computer simulation was used to investigate several techniques of generating liquid Cu targets. The target with the best liquid characteristics was subjected to one KeV, argon ion bombardment as a preliminary study of the sputtering of liquids. The techniques of warming by impulse and warming by initially displacing atoms from their equilibrium positions were compared. Both methods produced targets with good liquid properties. The energy became equally partitioned between kinetic and potential energy and all targets equilibrated within 400 fs. The range of a typical atom during the time of equilibration was found to be restricted to its initial neighborhood. The preliminary sputtering study resulted in a sputtering yield increase of 40% over the solid target, for a low index crystal plane.

.

TABLE OF CONTENTS

ACKNOWLEDGEMENTS

I would like to express my gratitude to the late professor Harrison of the Naval Postgraduate School. He introduced me to the topic of molecular dynamics in computer simulations and provided me with crucial guidance in the early stages of this investigation. He died before completion of the study but left me with a strong sense of direction and the willingness to see it through. I thank him for all his support, confidence and a very rewarding experience.

I would also like to thank my thesis advisor, Roger Smith for the time and effort he invested in this study at the expense of putting his own work aside.

I. INTRODUCTION

A. HISTORICAL OVERVIEW OF SPUTTERING

In 1851, Plucker [ref. 1] observed that the gas in x–rays tubes was continually removed. He attributed this phenomenon to the ionization of residual gases and their consequent absorption by the inner surface of the x–ray tube. In 1852, Grove [ref. 2] noticed that the x–ray tube surface struck by these particle ions was eroded due to the removal of target material. He called this phenomena *cathode sputtering.*

At that point in history, the action of target erosion or sputtering was considered undesirable in lab equipment, and was only interesting so long as one could minimize its unwanted effects. Consequently, sputtering was not investigated systematically for more than fifty years.

About fifty years after Grove reported his cathode sputtering findings, Goldstein [ref. 3] presented conclusive evidence that sputtering was indeed caused by the positive atoms of the discharge impacting on the cathode target.

In 1908, Stark [ref. 4] advanced the concept of the individual sputtering event on an atomic scale. He developed a collision theory which treated sputtering as a sequence of binary collisions initiated by the collision of one incident ion at a time. He also presented a second theory called the *hot–spot* model which attributed the sputtering action to localized high temperature heating of the target and evaporation of atoms. In 1921, Thompson [ref. 5] proposed that sputtering was caused by the release of radiation as the bombarding ions struck the target. The following year Bush and Smith [ref.6] suggested that sputtering was caused by the

1

expansion of gas adsorbed by the target material, and Kingdon and Langmuir [refs. 7,8] conducted a sputtering experiment which yielded ejecta from the surface layers of the target. They bombarded thoriated tungsten with ions in a glow discharge tube. The experiment demonstrated that the bulk of the ejecta was coming from the thin film of thorium on the target's surface instead of the tungsten substrate. Their results suggested a momentum transfer ejection mechanism for sputtering.

In 1926, Von Hipple and Blechschmidt [refs. 9–12], proposed a theory that described sputtering as an evaporation of the surface atoms. Von Hipple extended Stark's hot–spot model and attempted to formulate a sputtering theory on the basis of local heating. He expressed the view that local heating was the only feasible way to explicitly treat the statistics of the complex collisions occurring in a sputtering event.

Approximately ten years later, Lamar and Compton [ref. 13] published *A Special Theory of Cathode Sputtering* which led to the *thermal spike* concept. The thermal spike was based on momentum transfer between the incomming ion and the lattice atoms. This theory suggested that a long–lived high temperature volume persisted in the target even after the collision cascade was completed.

In 1931, Guntherschulze and Meyer [refs. 14,15] were the first to recognized the importance of minimizing ambient pressure in sputtering experiments. They used a high vacuum tube and took the precaution of removing several top layers from the target to clean its surface. Consequently, their results were the first to satisfy the conditions for reproducible sputtering yield determination. About ten years later,

2

Penning and Mobious [ref. 16] conclusively demonstrated the significant effects of ambient pressure on the sputtering yield.

By the early 1950's, a renewed interest in sputtering coalesced in the scientific community. This was brought about primarily by the fact that sputtering was found to have technological value. It was discovered that the ion–trapping process in sputtering could be used as a pumping effect for low pressure electronic systems. It was also found that sputtering could be used to clean target surfaces. Sputtering became useful to industry and its status was raised from that of a laboratory hindrance to one meriting serious scientific research effort.

In 1952, Keywell [ref. 17] formulated a sputtering theory which made use of existing neutron transport theories originally developed for nuclear reactor design. Keywell's work, as well as subsequent calculations by Harrison [ref. 18] made important contributions to the field of sputtering by introducing probability concepts in terms of collisional cross sections.

In 1954, Wehner [ref. 19] published his findings on crystal structure effects in the flux of sputtered particles. This was a significant advance in that it proved conclusively that Stark's hot–spot model was incapable of fully explaining the sputtering mechanism. Wehner's conclusions fortified collisional theory as an important part of sputtering theory. His findings created great interest in the collisional aspect of sputtering and served to point the way for following research efforts.

In the decade that followed, (mid 50's to mid 60's) the main emphasis in sputtering research was directed towards the study of crystal lattice effects. Such studies produced two main theories. These were the channeling theory and the

focusing collision theory. The channeling theory was successful in describing the angular variation of the yield when the incident ions where closely aligned to one of the target's principal axis or planes. The theory failed for general alignment of the incident ions. The focusing collision theory was the product of Silsbee [ref. 20]. His theory showed that momentum was transferred within the target's crystal structure along preferred directions. He introduced the idea of momentum transport without requiring mass displacement. This concept was later refered to as *focusons*. Focusing collision theory was relatively successful in modelling the observed ejection patterns from materials with a high degree of symmetry, such as cubic crystals, but only if bombarded with high energies. This theory, however, failed to match the Wehner spots and proved to be particularly inadequate for targets with low symmetry such as hexagonal crystal structures. Experimental results demonstrated that the sputtering yield was significantly dependent on the crystallographic orientation of the target with respect to the incident ion beam.

The theory of collisional cascades was further advanced by the work of Sigmund [refs. 21,22]. He used Lindhard's range theory [ref. 23] and proposed that for amorphous solids, the collision cascades could be described by a Boltzmann transport equation [ref. 24]. His equations required the target surface to have a disordered structure, not the long straight rows of atoms intersecting the surface used in the focusing model. He obtained first order asymptotic solutions for cascade events produced by ions of medium to large atomic number with energy in the KeV. His theory became the reference standard for sputtering yield measurements despite its limitation of application to polycrystalline solids with randomly oriented crystallites as an amorphous approximation. This idea was simultaneously

investigated by Thompson [ref. 25]. He proposed that the ejected atom was affected by the surface attraction of the target's surface, causing a deviation on the velocity vector of the outgoing particle. This resulted in a distortion of the angular distribution of ejected particles. Another important idea developed from collisional cascades was that of replacement collision sequences. In replacement collision sequences, the moving atom replaces an atom on its lattice site. The vacated atom the proceeds to strike and replace the next atom in the row. The sequence propagates as each atom replaces the next.

Despite its long history, sputtering researchers have not been able to formulate an analytical theory which can fully explain sputtering. There are still differences between the theoretical predictions and experimental data, and it seems that an analytically simple form, in all likelyhood, will not be sufficiently flexible to correctly describe all aspects of sputtering. The crux of the problem lies in the fact that in many cases, the theory requires the solution of a many–body problem with multiple interactions. This is a formidable task and one which historically has yielded, at best, only approximate solutions. Another approach was required which could explain and predict sputtering events based on a few simple laws. With the advent of the high speed coputer capable of handling the voluminous amount of required calculations, some researchers turned to computer simulations.

B. COMPUTER SIMULATIONS OF SPUTTERING

1. Historical Overview

By the late 1960's, the once curious laboratory observation of Plucker [ref. 1] and Grove [ref. 2], had been studied for approximately 100 years and

sputtering theories had evolved into dependable sputtering yield predictors. Especially successful in determining sputtering yield were the statistical theories of Thompson [ref. 25], ejected atom energy distribution function dN/dE, and Sigmund [ref. 24], sputtering yield as a function of energy, Y(E).

The advent of the high speed computer made it practical to perform the many calculations required to treat the collision cascade problem in a three dimensional crystal. And so, computer simulation made its debut in sputtering research.

A very important early computer simulation was the work of Gibson, et al [ref. 26] in 1960. They developed a computer model which simulated the motion of primary knock—on atoms in a copper monocrystal target. Their model assigned an arbitrary kinetic energy and direction to the struck atom as a means to simulate the collision effect. Atomic interactions were treated as binary collisions and the resulting motion obtained through Newtonian mechanics. Their results demonstrated the ability of computer simulations to isolate elementary sputtering prcesses for investigation. Two years later Robinson and Oen [ref. 27], utilizing a similar code, discovered the channeling effect. What makes this discovery so important is the fact that channeling had not yet been observed in the laboratory. For the first time, a computer simulation had predicted an important dynamic sputtering mechanism. Channeling was later verified experimentally.

In 1967, Harrison, Levy, and Effron [ref. 28] simulated the bombardment of a copper monocrystal by argon ions using repulsive pair potential interactions. Their findings demonstrated that the bulk of the sputtering yield came from the first three layers of the top surface. This model was later refined to include

attractive potential functions for the target [refs. 29–30]. This potential which includes attractive and repulsive interactions produced a dynamically stable crystal. In 1978 Garrison, Winograd and Harrison [ref. 31] published the result of a comprehensive simulation study of atomic and molecular ejection from a copper crystal with adsorbed oxygen atoms. The simulation provided a detailed description of the ejection mechanism. The results also allowed them to determine whether molecules were ejected as clusters or whether they combined together after leaving the target's surface. They also determined the effects of adatom placement on molecule formation.

In its short history computer simulation has successfully predicted and explained various specific sputtering events. Results of simulations have been both praised and strongly criticized by some theoreticians who argue that simulations neglect important factors. Nevertheless, the value of computer simulation has been recognized by the overall scientific community and it is now considered an important research area in the field of sputtering.

2.   General Concepts and Development

Most real systems are so complicated that a complete analytical description is virtually impossible to achieve. unfortunately, sputtering falls into this category of complexity.

The modelling of a real collision cascade such as a sputtering event is an attempt to describe a complex system in terms of idealized and highly simplified descriptors. Invariably, many factors must be neglected in order to simplify the model the selected set of descriptors must adequately determine the system's relevant behavior. Once this is achieved, the result is a simulation of a real system.

Computer simulations of atomic collisions allow researchers to concentrate on the basic physics of a system without the analytic constraints of statistical theories. It is a tool that can be used to test the applicability of a theory.

There are two major approaches used in computer simulations. These are the *time–step* and *discrete event* models. The discrete event model proceeds from event to event skipping over their time separation. It maintains a list of possible future events from which it determines the next event. This list is constantly being updated. This model works well when the events are sufficiently separated in time. In contrast, the time–step model advances the clock for a short interval first, and then computes all the interactions that occur in that time, updating all processes before the next time step. This model is the obvious choice for systems with simultaneous interactions. The time–step logic's chief drawback is that it requires significantly more computer running time than the discrete event program logic.

In sputtering applications, these two approaches lead to the two principal methods of simulation; the *binary collision* (BC) and the *multiple interaction* (MI) program logics.

The BC method [ref. 32] uses the discrete event model. The basic assumption of this type of simulation is that each particle interacts with only one other particle (usually assumed stationary) at a time. These simulations are inherentelly restricted to be linear calculations.

The multiple interaction simulation uses the time–step model and Newton's equations of motion are numerically solved for many particles. This is the method used in this thesis investigation.

C. SPUTTERING OF LIQUIDS

The sputtering of liquid targets has gained a great deal of attention in the scientific community. Experimental results of sputtering have shown that solid targets may undergo a phase transition to liquid under ion bombardment. Therefore, there is a practical as well as scientific interest to understand and be able to model the characteristics of a liquid surface.

1. Summary of Experimental Results

In 1962, Whener et al [ref. 33] reported their measurements on tin sputtered by argon ions. Their results showed a 40% larger yield for liquid tin at an ion energy of 0.2 KeV and a 6% smaller yield for an ion energy of 0.4 KeV. This was the earliest evidence of an energy dependent yield profile with a maximum sputtering yield peak. Eight years later Krutenat and Panzera [ref. 34] conducted a similar sputtering experiment on solid and liquid tin. Their results were in general agreement with those of Whener, showing that the solid yields below 0.2 KeV is twice that of the liquid and that a crossover occurs at 0.375 KeV above which the liquid yield is only 15% higher. Their results also implicated surface dynamics in sputtering mechanisms.

In 1982, Cooper and Hurst [ref. 35] bombarded liquid and solid indium with argon ions and discovered that above 0.107 KeV the liquid yield was 10% higher than the solid. They noted that the shape of the yield versus ion energy for both the liquid and solid were similar. They attributed the higher yield of the liquid to its lower binding energy.

Dumke et al [ref. 36] published their results on the sputtering of a gallium–indium eutectic alloy (surface monolayer greater than 94% indium) in the

liquid phase. Their findings indicated a ratio indium to gallium sputtering yield which was 28 times greater than expected from the stoichiometry. They were able to conclude that 85% of the sputtered atoms came from the surface monolayer.

2.   Historical Summary of Liquid Models

In order to study the effects of sputtering on a liquid surface using computer simulations, one first needs to develop a reasonable model of a liquid.

One very early model of a simple liquid was developed by Bernal in 1960 [ref. 37]. He stipulated that the structure of a simple liquid can be determined simply by volume exclusion. He then proposed a zeroth order model in which the atoms were considered hard spheres and their local structure determined by the restriction that no two atoms can approach each other by less than one atom diameter. Early Bernal models were constructed [refs. 38,39] by pouring thousands of steel balls into a deformable container (originally a football bladder). The ensemble was then bound with rubber strips and kneaded to maximize its density. The contents were then fixed by pouring melted wax into the container through holes and then allowed to solidify. The coordinates of each sphere were then individually and painstakingly measured (probably by one of his postgraduate students). This seemingly ad hoc procedure yielded a maximum hard–sphere non–crystalline packing of 0.6366. Amazingly, more recent attemts to reproduce this structure using modern computational techniques have at best produced indistinguishable results.

In 1968, Verlet [ref. 40] published the results of his computer experiments on classical fluids. His was one of the earliest attempts at modelling the liquid structure through a computer simulation. His model used a Lennard–Jones

potential as the means of particle interaction from which the equations of motion were solved. His study offered evidence that correlation functions at high density is due to the geometrical effects of a strong repulsion in the potential. He showed that the same behavior can be obtained by the approximate solution of the hard sphere problem and that the diameter of the hard spheres is the only parameter of the theory (in agreement with the simplistic Bernal model).

In 1982, Miranda and Torra [ref. 41] obtained good results for the liquid structure and for the self–diffusion constant with a computer simulation using functions derived from a local pseudopotential and various other dielectric functions.

3.   Computer Simulations Summary of Liquid Sputtering

In 1985, Lo et al [ref. 42] generated two liquid targets consisting of 603 copper atoms and then subjected them to an argon ion beam. The two targets differed only in the imposed boundary conditions. One target used a box boundary condition requiring particles to experience pure reflection at the boundaries and the other used a semi–periodic boundary condition requiring position and momentum periodicity in the two dimensions defined by the surface. They found that the semi–periodic boundary condition results were in better agreement with experimental sputtering results and concluded that such a target better represented the free surface of a real liquid. The target was warmed to liquid temperatures by assigning velocities to each atom with a random number generator. The target was then allowed to equilibrate for a few picoseconds. This energy imput scheme is particularly important to this research effort because it is used in generating one of our targets.

11

In 1987, Lo et al [ref. 43] again conducted a computer simulation study of collision cascades in liquid indium. Their results suggested that the detailed structure of the target surface layer is very important in the sputtering proccess.

The most recent simulation of liquid sputtering was done by Morgan [ref. 44]. He conducted a study of self—sputtering using a stratified liquid metal surface as a model. He observed an enhanced low energy yield which fell below those of other models for higher energies. These results appear to be in general agreement with various published measurements of liquid sputtering yields [refs. 34—36].

II. OBJECTIVES

This research and computer simulation effort has three specific objectives. The first objective is to develop a reasonable model of copper in the liquid phase by using a heavily modified version of QDYN (Quick Dynamics), a molecular dynamics computer program developed by Harrison [ref. 45]. The general intent, is to warm an fcc (copper) crystal by giving each atom in the crystal sufficient energy to reach liquid temperatures. The energy given to each atom is determined stochastically. The warmed ensemble is then allowed to interact through pair—wise forces until thermal equilibrium is reached at the desired liquid temperature. The resulting liquid targets will be compared to various known liquid—like characteristics such as the radial distribution function for copper in the liquid state and the expected Maxwell—Boltzmann (velocity distribution) function.

Eight different liquid targets will be generated using two different methods of warming (adding energy to the atoms) in combination with four different variations of dynamic integration. These variations are the permuted combinations of simulation runs with or without a reflective boundary condition and, or, with or without the requirement to update the nearest neighbor list in each time step.

The second objective is to compare the dynamic behavior of the two different warming methods. One of these warming methods is a variation of the method used by Lo et al [ref. 42], where the energy is added to each atom by assigning each

a random velocity. The second warming method was one suggested by the late professor Harrison of the Naval Postgraduate School. This involves warming a target by randomly displacing each atom from their stable positions and then allowing then to interact through pair–wise forces until equilibration is reached. Clearly, each method starts the molecular dynamics with a different form of excess energy. One method starts with excess kinetic energy and the other starts with excess potential energy. Therefore, the ability of QDYN to equilibrate the targets from such varying initial energy conditions will serve as further evidence for the applicability of pair–potentials in molecular dynamics.

The third objective is to use the resulting liquid targets in a computer sputtering experiment. The goal is to obtain sputtering yields which are in general agreement with published experimental data [refs. 33–36] as well as other liquid sputtering simulation results [refs. 42–44].

III. THEORY

A. LIQUIDS

Matter manifests itself in three states. One of these is the liquid state and is the least understood of all three. Understanding the unique descriptive characteristics of a liquid, especially those that may affect the interatomic collision process, such as density, radial distribution, velocity distribution and dynamic behavior, is of great importance to this research effort.

1. The Density of Liquids

The essential difference between a solid and a liquid is that a liquid is a much more disordered state [ref. 47]. A disordered ensemble of atoms requires more space than does a typical closed-packed and well-ordered crystal structure. Consequently, the density of a liquid structure can be expected to have lower density than that of a solid. In the case of copper, the density has been experimentally measured for a wide range of temperatures in the liquid phase and is found to linearly decrease with increasing temperatures. Cahill and Kisherbaum [ref. 48] have obtained experimental density measurements for copper from the melting point (1356 K) to 2500 K. Their results indicate that a plot of the density of copper versus temperature in the liquid phase can be accurately described by a straight line of negative slope given by,

$$\rho_1 = 9.077 - (8.006 \times 10^{-4} \; T_1)$$

where T_1 is the liquid temperature of copper in degrees Kelvin and ρ_1 is the density of copper in grams per cubic centimeter.

2. The Radial Distribution of Liquids

The liquid state imposes spatial restrictions on the possible ways that atoms can arrange to form amorphous structures. The nearest neighbors to a given atom cannot move too far away because of the repulsion force exerted by the other particles in the system. Due to these restrictions the liquid state has, on average, a very distinctive radial distribution as described by Azaroff [ref. 49]. This short range order of liquid makes it possible to describe atomic structure in terms of the average density of atoms per unit volume ρ_o and the actual density $\rho(r)$ a distance r away from an atom placed at the origin.

In monatomic liquids such as copper, the radial density is spherically symmetric and can be described as the number of atoms per unit volume contained in a spherical shell of radius r and of thickness dr around one atom designated as the origin. The volume of such a shell is the difference between the volumes of two spheres whose radii are r and r+dr. The density of atoms in such a shell is given by $4\pi r^2 \rho(r)dr$.

The radial distribution function for the atoms is defined as,

$$G(r) = 4\pi r^2 \rho(r).$$

The radial distribution, however, cannot be experimentally measured. Instead, the structure factor i(s), defined below, is obtained through x–ray or neutron diffraction experiments from which the radial distribution is calculated.

The radial distribution function $G(r)$ is related to the structure factor i(s) by the following Fourier transformation [ref. 50]:

$$G(r) = 4\pi r^2 \rho(r) = 4\pi r^2 \rho_o + \frac{2r}{\pi} \int_o^\infty s\ i(s)\ \sin(rs)\ ds$$

where ρ_o is the average density of the ensemble.

The problem with this transformation is that the values for i(s) must be known through ∞ . To avoid this problem, the method of Zei and Steffan [ref. 51] can be used to extend the range of measured i(s) without manipulating the experimental values. This is the method used by Eder et al [ref. 46] to obtain the radial distribution of liquid copper at 1393K and 1833K. This is the radial distribution against which the results of this simulation will be compared.

In computer simulations, the radial distribution is very easily obtained by tallying the actual separations of each atom from every other atom in the ensemble. This is the method used in our simulation. The distribution is normalized by dividing each bin total by the area of a shell whose radius is equal to the minimum distance of the bin. The reason for doing this is to better compare the distribution of a very small ensemble with that of a real system whose size is infinitely larger by comparison.

3.   The Velocity Distribution of Liquids

The general collision behavior of liquid particles as they interact through pair–wise forces is not very different from that of a gas. Therefore, we can expect a velocity distribution of a liquid to be similar to the velocity distribution of a gas.

The distribution of molecular speeds in a large sample of gas varies over a wide range of magnitude and has a characteristic distribution which depends on temperature. The first expression for the velocity distribution of a gas was derived out by Clerk Maxwell. According to Maxwell, a sample of gas containing N molecules has a distribution of velocities given by [ref. 52]:

$$N(v) = 4 \pi N_t \left[m/2\pi kT \right]^{\frac{3}{2}} v^2 \, e^{-(mv^2/2kT)}$$

where $N(v)dv$ is the number of molecules having speeds between v and v+dv, T is

17

the absolute temperature, k is the Boltzmann's constant, N_t is the total number of molecules and m is the mass of the molecule.

4.   Equilibrium and the Equipartition of Energy

The equipartition of energy theorem states that when the number of particles is large and Newtonian mechanics hold, all the energy terms have the same average value, and that the average value depends only on the temperature [ref. 52]. This means that the available energy distributes itself in equal shares to each of the independent ways in which molecules can absorb energy.

The energy given to the atoms by the warming scheme in the simulation will distribute itself into half kinetic energy and half potential energy. The energy going into kinetic will further distribute itself equally among the x, y and z components of kinetic energy. The energy is distributed through the many collisions that the atoms experience as the ensemble comes to equilibrium. The target is at equilibrium when the total added energy is completely partitioned.

A plot of the total kinetic energy versus time should resemble a damped sinusoid, oscillating about a value equal to half of the total added energy. A plot of the x,y and z components of kinetic versus time should show the components becoming equal as time progresses and their value approaches one sixth of the total added energy.

B. SPUTTERING

1.   General Concepts

Sputtering is the erosion of a target surface through the removal of atoms by the action of incident energetic particles. Sputtering occurs in nature when a hot

18

plasma, such as that found in a lightening bolt, comes in contact with a solid surface. Sputtering can be produced in the laboratory by subjecting a target surface to a plasma or a particle ion beam.

The most obvious measure of erosion effects is through the sputtering yield, Y, defined as the average number of atoms removed per incident particle. The yield is a function of target structure, target atom mass, incident beam alignment (relative to target structure), energy of incident particles and the mass of the incident particle. Sputtered particles can leave the target's surface with a broad distribution of energy, charge state and exit angles. In order to obtain reproducible experiments, the following conditions must be met [ref. 53]:

- The target surface must be clean.

- The gas pressure must be low enough such that the mean free path of ions and sputtered atoms is large.

- The ion current density must be high and the background pressure low so that formation of surface layers is prevented during the experiment.

- The ions must strike the target at a known angle.

- The energy spread of the incident beam must be small.

- The ionizing conditions in the ion source should minimize the production of multiple charged species; the atoms must be uniformly charged and separated.

- The lattice orientation of monocrystalline targets or texture of polycrystal must be known.

Sputtering theory has four major variants; collisional, thermal, electronic, and exfoliational. In this research effort, we are primarily interested in the collisional behavior of sputtering.

19

2.   Collisional Description

The collisional description of sputtering views the bombarding ions as energetic projectiles which deposit kinetic energy and momentum upon striking a target atom. This action is analogous to an atomic size game of billiards.

There are two main collisional processes; prompt collisional and slow collisional. Their name arises from their respective collision–event time duration. Once again we limit the scope of the research by concentrating on the prompt collisional process.

The prompt collisional process has a duration time of approximately 500 femtoseconds following impact. The general process occurs in the following manner; an incoming particle collides with a target atom and transfers some of its kinetic energy to it. If the energy received by the target atom exceeds the binding energy of its lattice site, a primary knock–on atom is created. This knock–on atom can travel through the target's lattice colliding with other atoms and transferring some of its kinetic energy and momentum. A near surface atom is sputtered if its kinetic energy has a component normal to the surface which is larger than the surface potential energy barrier.

There are four basic collisional sputtering descriptions; rebound, recoil, reflection, and direct or reflected recoil. these are summarized in turn in the following sub–sections.

a.   *Rebound Sputtering*

In the rebound sputtering sequence, an incident ion strikes an atom in the first atom layer. The atom initially receives a component of kinetic energy normal to the target surface and into the target. The atom then collides and recoils

off an atom in the second layer reversing the surface normal component of kinetic energy. The atom then escapes the surface through the first atom layer as illustrated by Figure 1 of Appendix A.

This mechanism applies only to adatoms which are much lighter than atoms of the substrate and assumes that atoms recoil without energy loss.

b. *Recoil Sputtering*

In the recoil sputtering process, the first atom struck by the bombarding particle is not the ejected atom. The bombarding particle imparts kinetic energy and momentum to an atom in the first atom layer in a collision process similar to the one described in rebound sputtering. The atom then undergoes a sequence of collisions with other target atoms as it plows inwards. The atom's initial inward component of kinetic energy is eventually turned back towards the surface through multiple recoil collisions. The atom finally strikes another atom from below causing its ejection from the surface. Often, only two collisions are required as illustrated by Figure 2 of Appendix A.

c. *Reflection Sputtering*

In reflection sputtering, the incoming ion is backscattered by a target atom below layer one. The reflected ion strikes an atom in layer one from below causing its ejection (see Figure 3 in Appendix A). This process is extremely rare due to the space and angle restrictions imposed by the lattice geometry.

d. *Sputtering by Direct or Deflected Recoil*

In direct or deflected recoil sputtering, an atom in any near–surface layer is struck by the incoming particle at grazing incidence. The struck atom is deflected by neighboring atoms, causing its ejection from the target surface. This process is illustrated by Figure 4 of Appendix A.

The four collisional sputtering mechanisms described above are simplified and highly idealized. What most often occurs in a sputtering sequence, however, is the formation of collisional cascades. When the first atom in a sequence is struck by the bombarding particle, it will undergo a series of collisions throughout the crystal structure until the atom exhausts its kinetic energy or it is ejected from the target structure. These multiple collision sequences allow many paths through which the initial ion energy can reach the surface of the target and cause sputtering or reach deep target atom layers and dissipate its energy as heat.

As a collision cascade develops, it may cause the sputtering of atoms through any of the mechanisms described above or a combination thereof. However, it is also possible for a cascade to produce no ejections at all. Such a cascade is illustrated by Figure 5 of Appendix A.

C. THE COMPUTER MODELS

1. Experimental Approach

a. *General Description*

The general approach to this study is to first obtain several reasonable liquid targets and then use the the best resulting target in a sputtering run. The first step is to generate a fcc(111) crystal lattice. This is done with the subroutine F111 [ref. 54]. Next, the atom ensemble is energized using a stochastic scheme. In this simulation, there are two distinct methods used to randomly assign energy to individual atoms. These will be individually discussed in later sections.

After the excess energy is given to the target, the dynamic part of the liquid simulation starts, and the atoms are allowed to interact through

pair–wise forces until they reach thermal equilibrium. This part of the simulation is done with a modified version of QDYN [ref. 45]. In sputtering simulations using QDYN, atoms are only assumed to move after collision with a moving atom, in generating the liquid all the atoms are designated as moving atoms from time–step one.

b. *Assumptions*

The most significant assumption is that the motion of particles in a liquid state can be approximated by pair–potential derived forces and that the particles obey Newtonian Mechanics. Another assumption (for sputtering) is that the atoms in a liquid target move so slow, compared to the ion and collision cascade atoms, that they can be considered static. The average velocity of liquid atoms at 1700K is about 670 m/sec. The average collision cascade atom is at least 10 times faster and the ion is almost 3000 times faster. A one KeV Argon ion moves at 3030 km/sec. So during a typical cascade lasting 300 fs the average liquid atom moves 2×10^{-2} m, approximately one half of a lattice unit.

2. Liquid Target Generation

The basic target consists of 1445 atoms originally placed at the lattice positions of an fcc crystal with a 111 plane orientation. The atom positions are defined in terms of lattice units. The lattice unit for copper is consistently used throughout the simulation as the basic unit of length. This unit, as well as other copper constants used in the simulation, can be found in Table 1 of Appendix B. The dimensions of the crystal are 19 x 8 x 17 lattice units.

The target is aligned in such a way that an incoming ion would strike the target in the 111 plane and travel in the positive y direction as illustrated by Figure 6 of Appendix A.

The atoms are warmed using two techniques as explained in the following sub-sections.

a.   *Warming by Impulse*

This method of warming atoms is a variant of the method used by Lo et al [ref. 42]. The general idea is to give each atom an initial impulse whose direction and magnitude is determined by a random number generator.

The warming is accomplished in two steps and each uses a different random number generator. The magnitude of velocity for each atom is obtained from the product of a multiplicative constant (the speed of interest) and a set of random numbers having a Gaussian distribution about unity with a standard deviation of one. The random numbers were scaled to go from zero to two. This was done to avoid large velocities. The multiplicative velocity constant is chosen to be the velocity corresponding to twice the desired kinetic energy. This is done to allow for the equipartition of half of the added energy into potential energy elements. In our case, the desired temperature is 1462 K. Therefore, the velocity corresponding to twice the temperature is 1067.7 meters per second. This is the multiplicative constant used in the generation of random speeds. The individual atom velocities are the products of this speed with a series of random numbers.

The direction of each atom must be uniformly distributed in 3-D space. The velocity directions are obtained from the sines and cosines of a spherical

coordinate system. The sines and cosines are obtained from a random number generator which produces uniform random numbers between zero and one.

The actual warming is done by a subroutine called "warm", excerpt of which is shown below,

```
            SUBROUTINE WARM
            PARAMETER(LTMX=1854)
            DIMENSION RAN(LTMX),VRAN(LTMX*5)
              .
              .
              .
            DO 300 I=1,LT
            R1=VRAN(I)
            R2=VRAN(I+(2*LT))
            R3=VRAN(I+(3*LT))
            R4=VRAN(I+(4*LT))
            R5=VRAN(I+(5*LT))
            VELMAG=VMAG*RAN(I)
            SIGN1=+1.0D0
            IF(R5.LT.0.5D0)SIGN1=-1.0D0
            SIGN2=+1.0D0
            IF(R5.LT.0.5D0)SIGN2=-1.0D0
            COSPHI=SIGN2*R1
            SINPHI=DSQRT(1.0D0-COSPHI*COSPHI)
            SINTHE=SIGN1*(2.0D0*R3*R4)/(R3*R3+R4*R4)
            COSTHE=(R3*R3-R4*R4)/(R3*R3+R4*R4)
            VX(I)=VELMAG*(SINPHI*COSTHE)
            VY(I)=VELMAG*(SINPHI*SINTHE)
            VZ(I)=VELMAG*COSPHI
  300       CONTINUE
              .
              .
              .
            CONTINUE
            RETURN
```

This do–loop goes from 1 to LT, where LT is the total number of atoms. VELMAG is the velocity magnitude of each atom I, obtained from the product of a velocity multiplicative constant, VMAG, and a random number RAN(I). The vector RAN(I) is a set of random numbers with a gaussian

distribution about unity and with a standard deviation of one. These numbers are not allowed to be greater than two or less than zero to avoid large velocities. R1–R5 are uniformly distributed sets of random numbers obtained from the vector VRAN(I). R2 and R5 are used to define the sign(+/–) for SINTHE and COSPHI. COSPHI, SINPHI, SINTHE, and COSTHE are the sines and cosines of the usual spherical coordinate directional angles φ and σ. VX(I), VY(I), and VZ(I) are the resulting components of velocity for atom I.

The liquid simulation program using this type of warming technique is called QLV.

b.   *Warming by Displacement*

This warming scheme gives added potential energy to the ensemble by individually displacing each atom away from their positions of minimum potential. The displacement is assigned to each atom by adding multiples of the thermal amplitude to the x,y and z components of position. The individual component displacement is the product of the thermal amplitude and a random number. The random number generator used produces numbers which are Gaussian distributed about zero and with a standard deviation of one.

The thermal amplitude, T_{amp}, is obtained from the relation,

$$T_{amp} = \sqrt{\overline{u^2}}$$

where $\overline{u^2}$ is the mean square of total displacements of an atom from the average position. This is a value which can be experimentally obtained.

The existing experimental measurements of $\overline{u^2}$ are for temperatures well below the liquid phase. For this reason, the warming must be done in cycles.

Each atom is displaced several times until a suitable liquid temperature is achieved. The first warming cycle consists of displacing all atoms from their equilibrium positions by adding to each component of position a random multiple of a known thermal amplitude. The following warming cycles further displaces each atom from their last position using the same principle. The warming behavior of such sequential cycling is that a maximum average temperature is reached after several cycles. Further displacements cause the total energy to oscillate about some average.

The thermal amplitude corresponding to 300K was chosen because it was an actual data point in the experimental results of Singh and Sharma [ref. 55]. The corresponding thermal amplitude used in the simulation is 0.0782 lattice units. The liquid simulation program using this type of warming technique is called QLP.

c.   *Achieving Thermal Equilibrium*

Thermal equilibrium is achieved by allowing the atoms to interact with each other through pair—wise forces. The target is considered to be in thermal equilibrium when the plot of kinetic energy versus time settles at half of the total added energy and the x,y and z components settle at equal values. Since the added energy in the impulse—warmed program starts with all kinetic energy and the displacement—warmed program starts with all potential energy, the plots of kinetic energy versus time for QLP and QLV resemble mirror images. These plots are similar to damped sinusoids which approach the value of half of the total added energy as the target comes to equilibrium.

d.   *Boundary Conditions*

Simulations were run with and without boundary conditions. The boundary conditions requires the atoms to experience pure reflection at the boundaries. The target boundaries for reflection are the uniformly expanded solid crystal dimensions corresponding to a liquid density. The density of copper is obtained from the experimental measurements of Cahill and Kirshenbaum [ref. 48].

The simulation programs were also run without boundary conditions to investigate the extent of the overall system expansion due to the interatomic interactions.

3.   Sputtering Program

The computer program used for sputtering is SDYN88A, and it is a variant of QDYN developed by Harrison [ref. 45]. The program uses *multiple−interaction* (MI) logic in a *time−step* approach.

The following actions occur in each time−step;

- Summation of pair−wise forces for each atom.
- Calculation of new velocities and positions.
- Movement of atoms to their new positions.
- Test energy conservation.

The forces affecting individual atoms are not computed until a collision occurs. This initial collision turns the atoms on (designates them as moving atoms) and puts them on a moving−atom list. Once in this list, the atom's interactions are computed each time step.

The moving atoms maintain a list of the atoms with which they can interact. This list is called the *nearest neighbor list*. The process of updating this

list requires considerable computing time. For this reason, it is updated every five time steps.

The forces are computed by solving Newton's equations of motion. A predictor–corrector integration scheme adjusts the time increment of each time step based on the fastest atom. The integration technique is unique in that position and velocity are calculated for the same instant of time.

The program was originally designed to study the effects of sputtering in solid targets. Consequently, the original logic did not calculate the new velocities and positions of every atom each time–step. Instead, only the moving atoms were updated. In our version, however, all of the target atoms have velocity from the start of dynamic integration. The initial atom positions and velocities are read from an input file created by the liquid simulation programs QLP and QLV.

In order to study the validity of using a static target in liquid sputtering simulations, we have allowed for the simulation to proceed with either the atoms turned "on" or "off". When the atoms are turned on, the simulation assumes every atom in the target is moving. When the atoms are turned off, the individual atom velocities are zeroed until they undergo a collision with a fast atom or ion. Such static targets are the equivalent of an amorphous solid with liquid densities. The computing time for a run with the atoms turned on is about five times greater. The justification for using a static target is that the velocity of a 1KeV ion is much faster than that of an atom in the liquid state (about 3000 times faster for 1700 K). The average velocity of a Cu atom in the liquid state is about 800 m/sec. The collision cascade atoms are about 10 times faster than liquid atoms.

The ion impact points are determined by a grid of 300 irregularly spaced points. The grid is one lattice unit squared. The grid is overlaid near the center of the target. For our target the grid reference point was chosen as x=6.25 LU and y=11.5 LU. The impact point coordinates are read in from the input file and added to the reference position.

D. POTENTIAL FUNCTIONS

1. Background

If we take two atoms originally separated by a large distance and slowly bring them together, the atoms will eventually start to experience an attractive force. This attraction can be simulated with an attractive potential function that has the characteristics of a *well*. As the particles get closer, the potential decreases until the point where the force changes from attractive to repulsive. This point corresponds to the equilibrium separation. As the pair gets closer together, the repulsive force quickly increases. This is known as the hard collision range. The potential in this range has the characteristics of a *wall*.

In the simulation, the molecular dynamic interactions are caused by two—body forces. The basic assumption is that the forces and potential energies depend solely on the physical properties of the interacting particles and their internuclear separation. The individual pair—wise interactions that each atom experiences due to its neighbors is summed to obtain the resultant force for that particle.

The range of the attractive force for Cu—Cu is assumed to be 2.4 lattice units. This range corresponds to a point between the second and third nearest

neighbors. This range cut–off has been investigated and found to be reasonable for fcc targets [ref. 56]. The differences in potential beyond the second nearest neighbors were found to be minor.

2. General Forms

The atom–atom potentials are composite functions consisting of a repulsive section, the *wall*, joined smoothly to an attractive section, the *well*. The joining of the two functions is accomplished by a cubic spline function. The atom–ion potential is a strictly repulsive wall, which is much steeper than that of the atom–atom.

The atom–atom repulsive wall is a Born–Mayer potential function given by [ref. 57],

$$V(r) = A\ e^{-Br}$$

where A is the atom's hardness and B is the atom's size.

The atom–ion repulsive wall is a Moliere potential function given by,

$$V(r) = [(Z_1 Z_2\ e^2/a)/(r/a)]\varphi(r/a)$$

where

- $\varphi(r/a) = [0.35e^{-0.3r/a} + 0\ 55e^{-1.2r/a} + 0.1e^{-6.0r/a}]$

- $a = 0.8853a_o\left[\sqrt{Z_1} + \sqrt{Z_2}\right]^{-2/3}$
- a_o = Bohr radius

- Z_1 = atomic number of atom

- Z_2 = atomic number of ion.

The general form used for the well is a Morse potential of the form,

$$V(r) = D_e[\, e^{-<2\alpha(r-r_e)>} - 2e^{-<\alpha(r-r_e)>}]$$

where

- D_e = well depth

- r_e = equilibrium separation

- α = well width control.

1. The Functions Used in the Simulation

The atom–atom potential is a repulsive Born–Mayer joined to an attractive Morse potential by a cubic spline.

The composite pair potential function is given by,

$$V_{ij} = A\, e^{-Br} \hspace{6cm} r \leq R_a$$
$$V_{ij} = C_o + C_1 r + C_2 r^2 + C_3 r^3 \hspace{3cm} R_a < r < R_b$$
$$V_{ij} = D_e[\, e^{-<2\alpha(r-r_e)>} - 2e^{-<\alpha(r-r_e)>}] \hspace{1.5cm} R_b \leq r < R_c$$
$$V_{ij} = 0 \hspace{7cm} R_c \leq r$$

where V_{ij} is the composite potential for the ith and j^{th} atom separated by a distance r.

The cubic spline joins the Born–Mayer and Morse at points R_a and R_b. The attractive Morse function is truncated at R_c, between the second and third nearest neighbors.

The atom–ion potential is obtained with the purely repulsive Moliere function,

$$V_i = [(Z_1 Z_2\, e^2/a) \, / \, (r/a)]\, \varphi(r/a) \hspace{2cm} r < R_a$$
$$V_i = 0 \hspace{7cm} r \geq R_a$$

where V_i is the potential of the ith atom and the ion.

The potential function parameters used in the simulation are found in Table 2 of Appendix B. The cubic spline parameters are found in Table 3 of Appendix B. The actual Ar–Cu and Cu–Cu potential functions are plotted in Figures 7 and 8 of Appendix A.

E. ERROR ANALYSIS

1. The Experimental Error

Since the system is non dissipative, energy is conserved and the energy calculation results may be used as a possible check of numerical error. In sputtering simulations, a small percent of energy error (up to 3%) is considered acceptable. The justification is that studies have shown that a small change in the initial ion energy does not significantly affect the sputtering yield. In the simulation of a liquid, however, the conservation of energy is an important factor which should be maintained.

The principal reason for our concern with energy conservation is that an error in energy is related to an error in temperature by,

$$\text{energy error} = 3/2Nk \text{ x temperature error}$$

where N is the number of particles and k is the Boltzmann constant.

This equation says that a 1 eV uncertainty in energy corresponds to a maximum uncertainty in temperature of 5.35 K. This means that a 1% error in the total energy of a liquid target, say 2461 eV, equilibrated to a temperature of 1575 K would correspond to an uncertainty in temperature of ± 65.95 K. Such an uncertainty in temperature would be critical if the temperature of the liquid is close to either the melting or boiling points. The largest energy loss in the simulation was 6.45 eV with a corresponding temperature uncertainty of 34.51 K.

2. Establishing the Fit of Curves

According to Maxwell's equipartition of energy, the energy added to a number of molecules will be equally partitioned between the potential energy and the components of kinetic energy as the ensemble comes to thermal equilibrium. The variation of total kinetic energy with time is, therefore, a good indicator of thermal equilibrium. In our simulation, when the total kinetic energy approaches a value equal to half of the total added energy and when the components of kinetic energy become more or less equal, the group of atoms will be considered to be in thermal equilibrium. How close these relationships come to their theoretically expected values will be the principal measure of target equilibration.

The third type of relationship generated from the results of the liquid simulation programs is the radial distribution of the atoms. This has been determined experimentally [ref. 46]. The calculated radial distribution function will be compared to the experimental radial distribution function by the general shape and by the coincidence of their peaks and valleys.

The velocity distribution can be compared to the theoretical expected value using statistical analysis. The expected distribution of the atom velocities is the Maxwell–Boltzmann distribution. χ^2 tests will be used to determine how well the calculated velocity distributions fit the expected theoretical values of the Maxwell–Boltzmann distribution function. The following equation is used to obtain the χ^2 values,

$$\chi^2 = 1/d \sum_{k=1}^{n} \frac{(O_k - E_k)^2}{E_k}$$

34

where

- d = number of degrees of freedom
- $k = 1 \cdots n$, individual number of bins
- O_k = observed values
- E_k = expected values.

Generally, if $\chi^2 \gg 1$, the observed results do not fit the assumed distribution very well. The fit is generally considered acceptable for a $\chi^2 \leq 1$.

A more qualitative measurement of the fit is made by finding the percentage probability $P_d(\chi^2 \geq \chi_o^2)$ of obtaining a value of $\chi^2 \geq \chi_o^2$. Where χ_o^2 is the actual value of χ^2 obtained from experimental measurements. These probabilities are found in Table D, page 251 of reference 58. If the probability $P_d(\chi^2 \geq \chi_o^2) \leq 5\%$ then the fit is considered to be acceptable. This is the criteria applied to our results.

In our simulation, the number of bins used for the velocity distribution is 30 and the degrees of freedom is $d = 29$. Using Table D of reference 58, the maximum χ^2 corresponding to a $P_d(\chi^2 \geq \chi_o^2) = 5\%$ for 29 degrees of freedom is 1.493. Therefore, if the χ^2 of any of our velocity distributions is under 1.493, then the fit will be considered to be consistent with the expected values.

IV. RESULTS AND DISCUSSION

Eight different targets were generated using various boundary conditions, warming methods and nearest neighbor list update schemes. The target with the best liquid–like characteristics was chosen and subjected to a 295 trajectory sputtering run.

In order to facilitate reference to the various simulation schemes and their results the following names are defined,

- QLP, Liquid simulation using the atom displacement warming scheme and unrestrained boundaries.

- QLPBC, Liquid simulation using the atom displacement warming scheme and reflective boundary conditions.

- QLP–REV1, Liquid simulation using the atom displacement warming scheme, unrestrained boundaries and a new neighbor–list update every time step.

- QLPBC–REV1, Liquid simulation using the atom displacement warming scheme, reflective boundary conditions and a new neighbor–list update every time step.

- QLV, Liquid simulation using the impulse warming scheme and unrestrained boundaries.

- QLVBC, Liquid simulation using the impulse warming scheme and reflective boundary conditions.

- QLV–REV1, Liquid simulation using the impulse warming scheme, unrestrained boundaries and a new neighbor–list update every time step.

- QLVBC–REV1, Liquid simulation using the impulse warming scheme, reflective boundary conditions and a new neighbor–list update every time step.

36

BC means that reflective boundary conditions are applied and REV1 stands for the revision which includes the update of the nearest neighbor list every time step.

A. ENERGY CONSERVATION

The calculated total energy losses for all eight runs range from 0.001% to 0.25%. The equivalent energy uncertainty for this range is 0.03 eV to 6.45 eV. Although all eight results have acceptable energy losses, there is a clear division in the energy conservation efficiency betweeen the runs that update the nearest neighbor list every time step and those that do not. The simulation runs which update the nearest neighbor list each time step give the poorest energy conservation. This is to be expected because as the simulation proceeds, atoms find new neighbors with which they can interact and this requires additional calculations that add to the total error.

The best energy conservation was obtained with QLPBC. A summary of the experimental error for all eight targets is found in Table 4 of Appendix B.

B. DENSITY RESULTS

The density was calculated for each of the unrestrained targets (without reflective boundary conditions) after equilibration was reached. These were found to be slightly lower than those corresponding to liquid copper at the equilibration temperature.

The most accurate density was obtained with QLV–REV1. This simulation yielded a liquid density of 7.664 gm/cm^3, within 1.8% of the expected value for a liquid temperature of 1690 K. Table 5 of Appendix B shows the resulting densities for all runs with unrestricted boundaries and their expected theoretical values.

C. TARGET EQUILIBRATION AND FINAL TEMPERATURES

The plots of total kinetic energy versus elapsed time (Figs. 9–16, Appendix A) and those of the components of kinetic energy versus elapsed time (Figs. 17–24, Appendix A) show that all targets reach equilibrium after approximately 400 femtoseconds. No significant change in the kinetic energy or in the components of kinetic energy is observed after this time. This equilibration time seems to be consistent with the simulation results of Lo et al [ref. 42]. The simulations were computed for at least twice the equilibration time.

These kinetic energy plots also show that equipartition of energy holds very well for all eight target generation schemes. In particular, QLPBC produced a final kinetic energy of 273 ± 17 eV, less than 1 eV difference from the theoretical expected value of 273.071. The error for the total kinetic energies is taken from the maximum amplitude of the kinetic energy oscillations about an average value following the equilibration point. Table 6 of Appendix B summarizes the final kinetic energy and temperature results for all eight targets.

QLV–REV1 and QLVBC–REV1 produce the smallest kinetic energy oscillations at equilibrium, ±4 eV. This corresponds to a temperature uncertainty of ±32 K. The final temperatures for these two targets are 1690 ± 32 K and 1700 ± 32 respectively. The reason for such oscillations in kinetic energy after equilibration is reached is that the size of the ensemble is small compared to a real liquid system. Real systems have many billions of particles and the total kinetic energy fluctuations can average out.

D. RADIAL DISTRIBUTIONS

The radial distribution for an unwarmed solid copper crystal is given by Figure 25 of Appendix A. A comparison of this figure with the various radial distributions produced by the liquid simulations (Figs. 26–33 of Appendix A) clearly contrasts the structure differences between a solid and a liquid. These liquid radial distributions have the distinctive wide and smooth, peaks and valleys characteristic of a liquid. The crystal structure is completely lost in all samples.

The peaks and valleys of all the resulting radial distributions are compared against each other for consistancy, and against neutron diffraction experimental results [ref. 46] for validation, in Table 7 of Appendix B. All the numbers for this table are taken directly from the radial distributions plots, Figures 26–33 of Appendix A. It is important to note that many of the expected valleys could not be positively identified and were therefore left blank.

The best (most liquid–like) radial distributions are those obtained with QLP–REV1, QLPBC–REV1, QLV–REV1, and QLVBC–REV1. These radial distributions are in excellent agreement with the neutron diffraction experimental results [ref. 46]. The very best radial distribution of all is that of QLVBC–REV1.

E. VELOCITY DISTRIBUTIONS

The resulting velocity distribution and the expected Maxwellian distribution for each target are plotted together in Figures 34–41 of Appendix A. These figures show that the velocity distribution of all eight liquid targets generally match the Maxwellian distribution. The reduced χ^2 tests and their probabilities $P_d(\chi^2 \geq \chi_0^2)$ are

found in Table 8 of Appendix B. This table shows that the most Maxwellian–like velocity distribution is obtained with QLP. Only three targets QLP, QLV and QLVBC–REV1 have velocity distributions with a $P_d(\chi^2 \geq \chi_0^2) > 5\%$. This is the standard rejection criteria. The smallest $P_d(\chi^2 \geq \chi_0^2)$ was 0.5% with most falling around 1.5%. In general, the velocity distributions appear to be consistent with the Maxwellian distribution.

F. SPUTTERING RESULTS

The QLVBC–REV1 target was chosen for the sputtering run because it has the best overall liquid–like characteristics. 295 trajectories were run with 1.0 KeV argon ions. The liquid target atom velocities were zeroed to save both computational costs and real time running requirements. A sputtering run with live atoms (all atoms initially moving) takes on average about five times longer than a static target.

The sputtering program had on average a 3% energy loss per trajectory. Although this is considered acceptable for a sputtering simulation, it was later found that the program overestimated the amount of energy that left the target with every ejected atom, but did not affect the forces. Thus 3% is very much an upper bound.

The final average yield for the 295 trajectories is 8.28 atoms per incident ion. This is 40% higher than the typical yield expected from a solid target on the 010 face and at room temperature. This increase in yield is in qualitative agreement with experimental results [refs. 33–35] and with another computer simulation [ref. 43]. Table 9 in Appendix B shows the general consistancy of these results.

V. CONCLUSIONS

Results from the various liquid target generation schemes have shown that the warming method used to energize the individual target atoms does not affect the final liquid–like characteristics of the resulting target. That is, results of liquid targets warmed by impulse were essentially indistinguishable in radial distribution and in velocity distribution from those warmed by displacement. Both warming methods are equally capable of generating liquid targets.

The best results were obtained with the application of reflection boundary conditions in conjunction with a scheme which updated the nearest neighbor list every time step. QLPBC–REV1 and QLVBC–REV1 produced good liquid targets. The liquid target generated by QLVBC–REV1 is found to be the best of the two. Figure 43 shows the actual liquid structure generated by QLVBC–REV1. The straight lines in this figure represent the outline of the crystal before warming and equilibration.

Results indicate that the motion of a typical liquid atom in a time span equivalent to at least twice the equilibration time (approximately 800 fs) is such that it seldom leaves its original atom neighborhood. Figure 42 in Appendix B illustrates this behavior.

The sputtering of the best liquid target with a 1 KeV incident argon ion resulted in yields which were 40% higher than expected by solid targets. This is in qualitative agreement with the results of other experimental efforts [refs. 33–35] found in Table 9 of Appendix B. Figures 44 and 45 in Appendix A show the yield per incident particle distribution for both a crystal Cu(010) target and a Liquid Cu

41

target respectively. The large number of trajectories that have no yield at all for the crystal target may be attributed to ion channeling.

The spot pattern (spatial distribution of ejected material) of the liquid target, Figure 46, shows no signs of an ordered structure. The spot pattern of a Cu(010) crystal, Figure 47, is shown to contrast the difference in spot pattern between a well ordered structure and an amorphous ensemble.

In summary, the liquid target generation methods QLVBC–REV1 and QLPBC–REV1 both produced reasonable liquid targets. The frequent update of the nearest neighbor list as well as the application of boundary conditions was found to be critical in making a reasonable liquid structure. The sputtering results are in general agreement with published data.

VI. RECOMMENDATIONS

The primary purpose of this investigation was to devise a method that would produce a reasonable liquid target. This was achieved.

The secondary objective was to conduct a preliminary study of liquid sputtering using the best liquid target. The average sputtering yield was obtained from a set of 295 trajectories using only one liquid target. Other targets should also be used in sputtering runs in order to obtain additional evidence for the validity of the liquid targets. It is possible that by using the same liquid target for every trajectory we may be introducing a systematic bias in the sputtering yield. It is reasonable to assume, for example, that our yields are closer to that of an amorphous solid than that of a liquid because the target has constant structure.

A scheme should be devised by which several equivalent liquid targets are used in turn (cycled) with each trajectory of a full sputtering run. Another alternative would be to complete several sets of trajectories on sufficiently separated areas of the surface.

At least one liquid target should be subjected to various ion energies to determine if there is an energy dependent yield profile as suggested by the results of reference 33. The effect on yield by varying the angle of incidence should also be investigated.
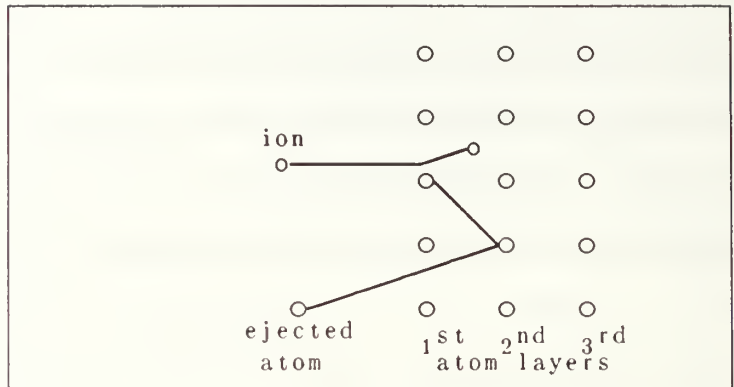
Figure 1. The Rebound Sputtering Process
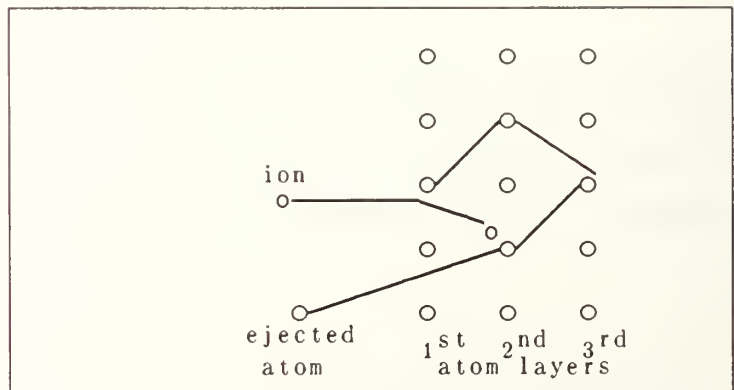
Figure 2. The Recoil Sputtering Process
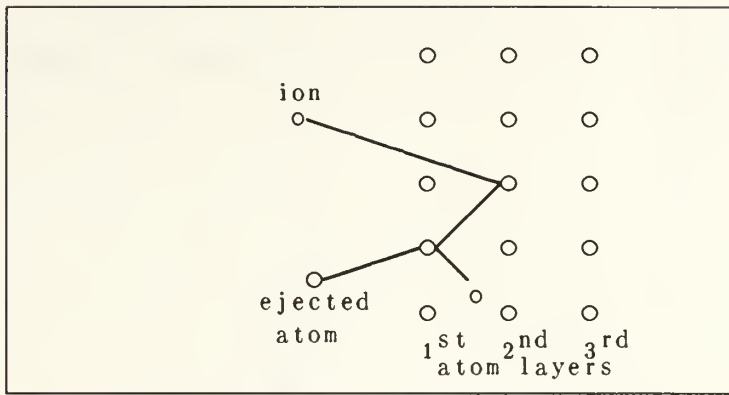
Figure 3. The Reflection Sputtering Process
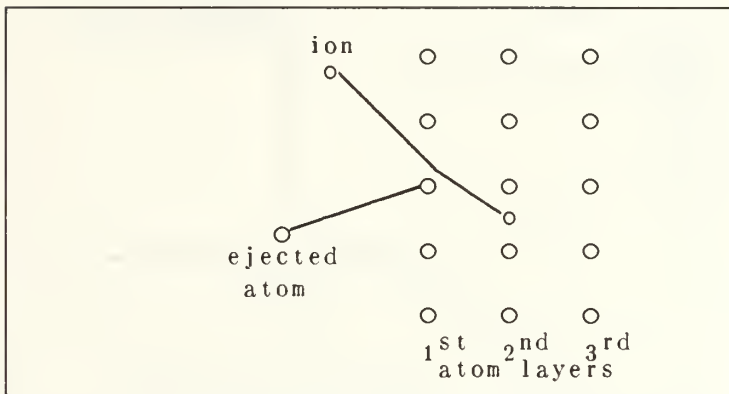
Figure 4. The Direct or Deflected Recoil Process
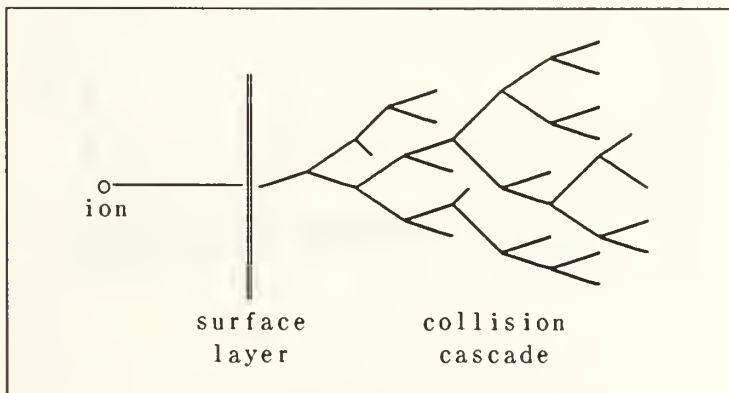
Figure 5. The Collision Cascade

45
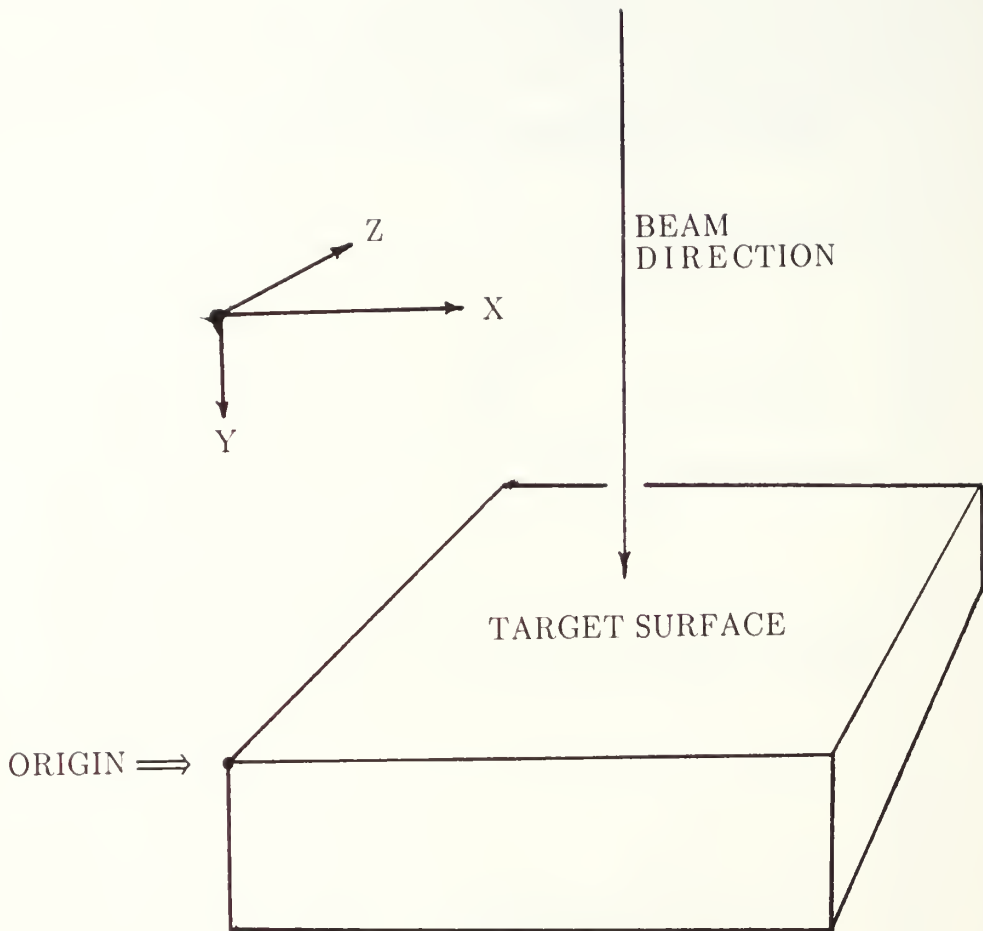
Figure 6. The Target—Ion Alignment.

Figure 7. Ar–Cu Potential Function.

47
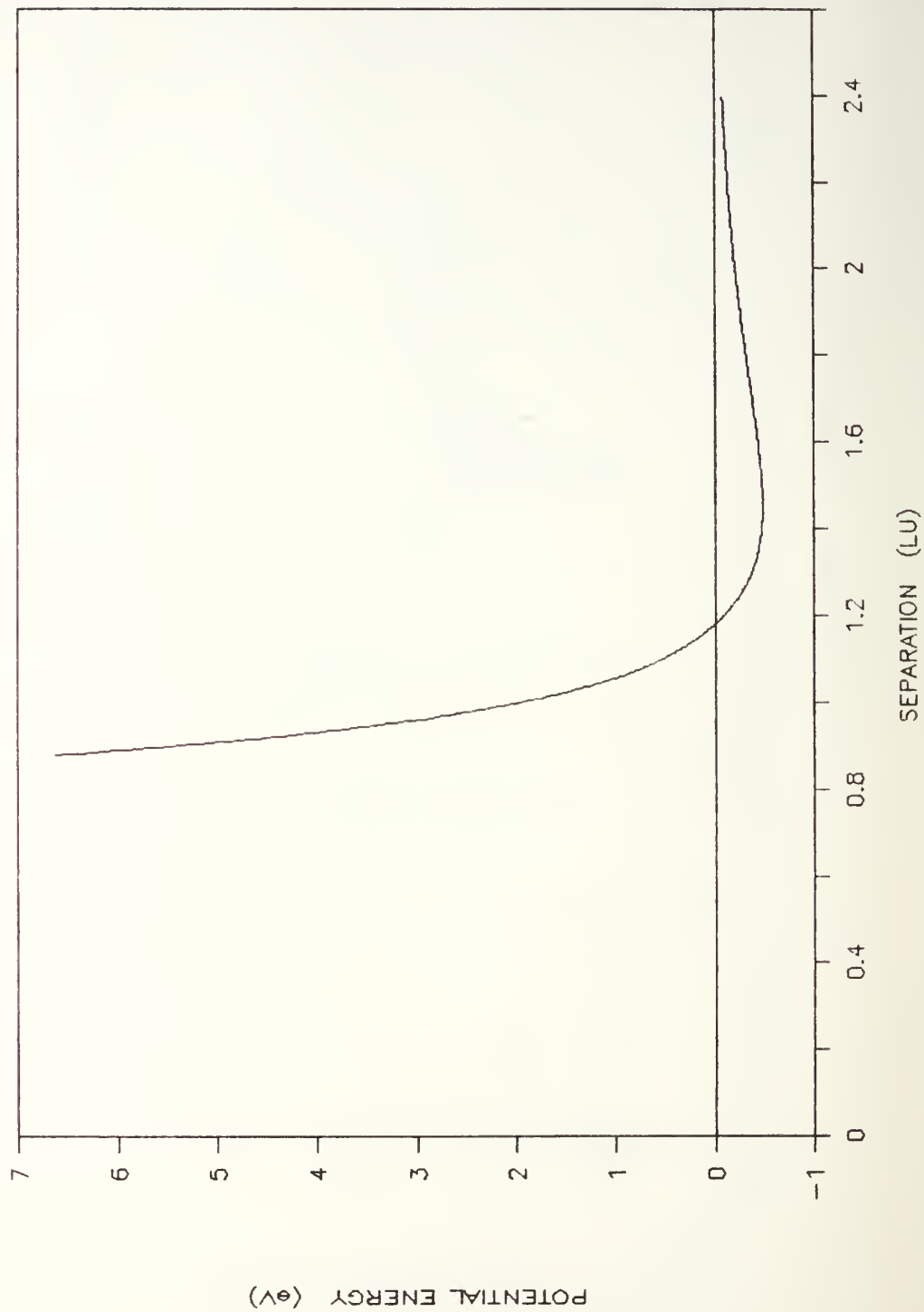
Figure 8. Cu–Cu Potential Function.
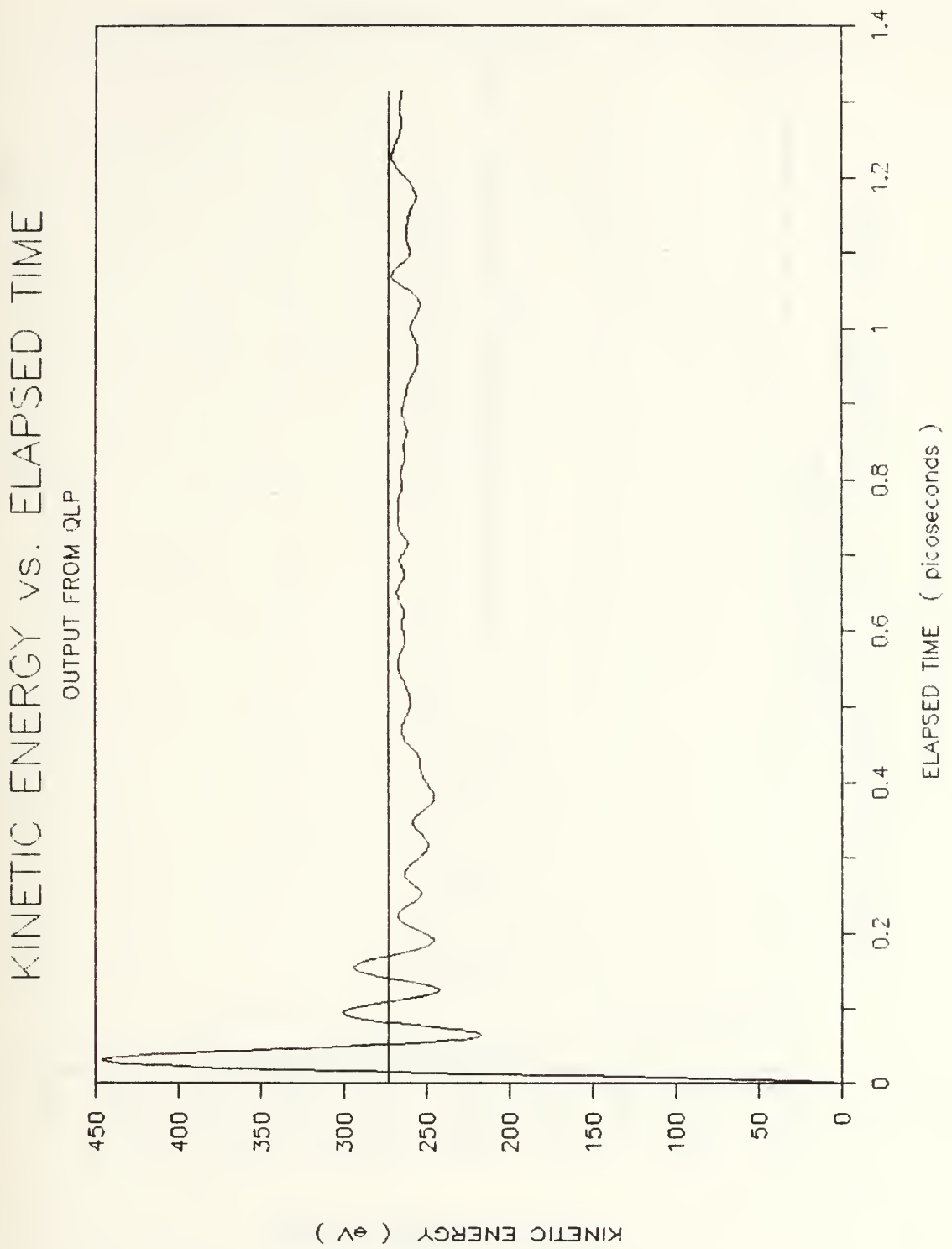
Figure 9. Kinetic Energy Versus Elapsed Time, QLP Output.

49
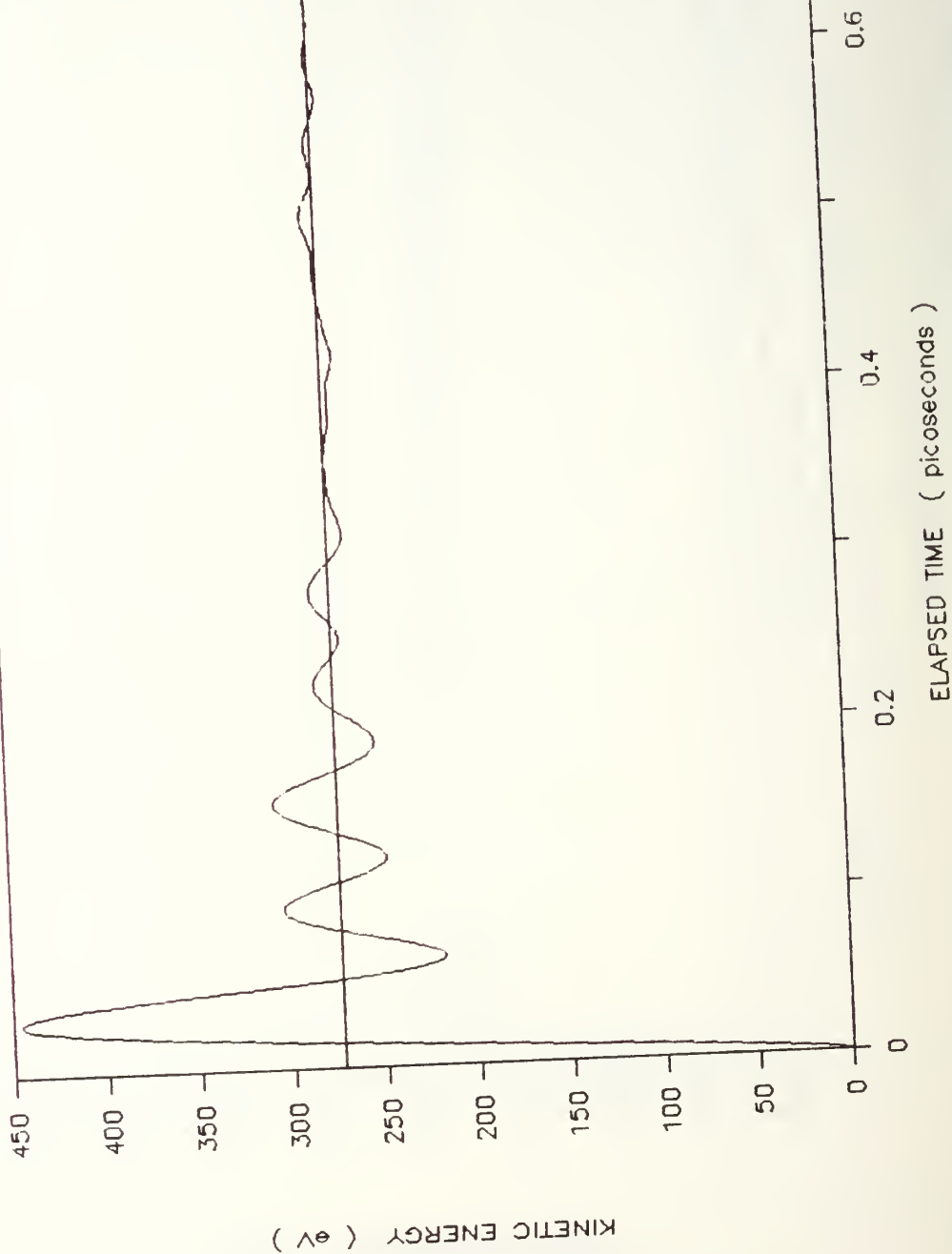
Figure 10. Kinetic Energy Versus Elapsed Time, QLPBC Output.

50
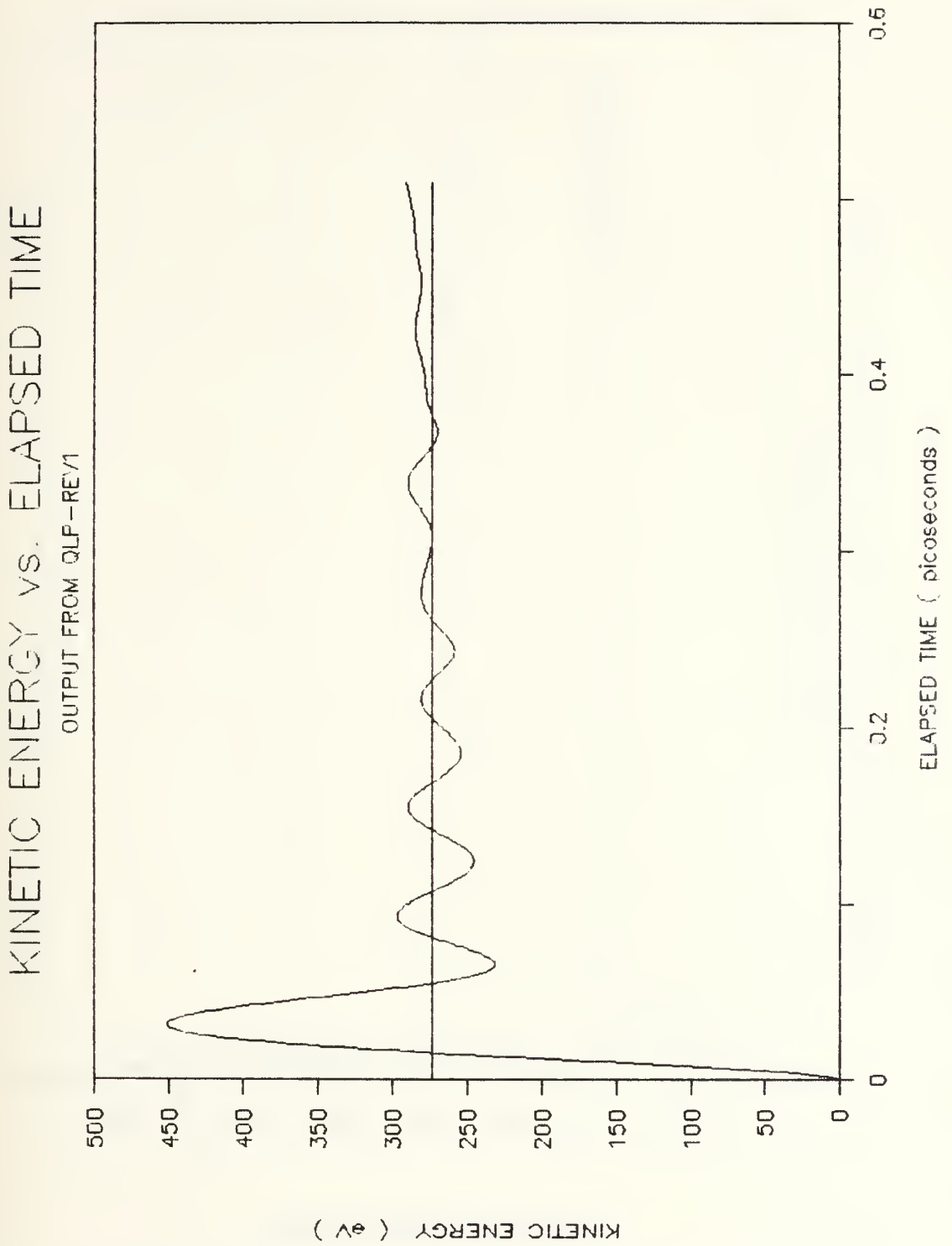
Figure 11. Kinetic Energy Versus Elapsed Time, QLP—REV1 Output.
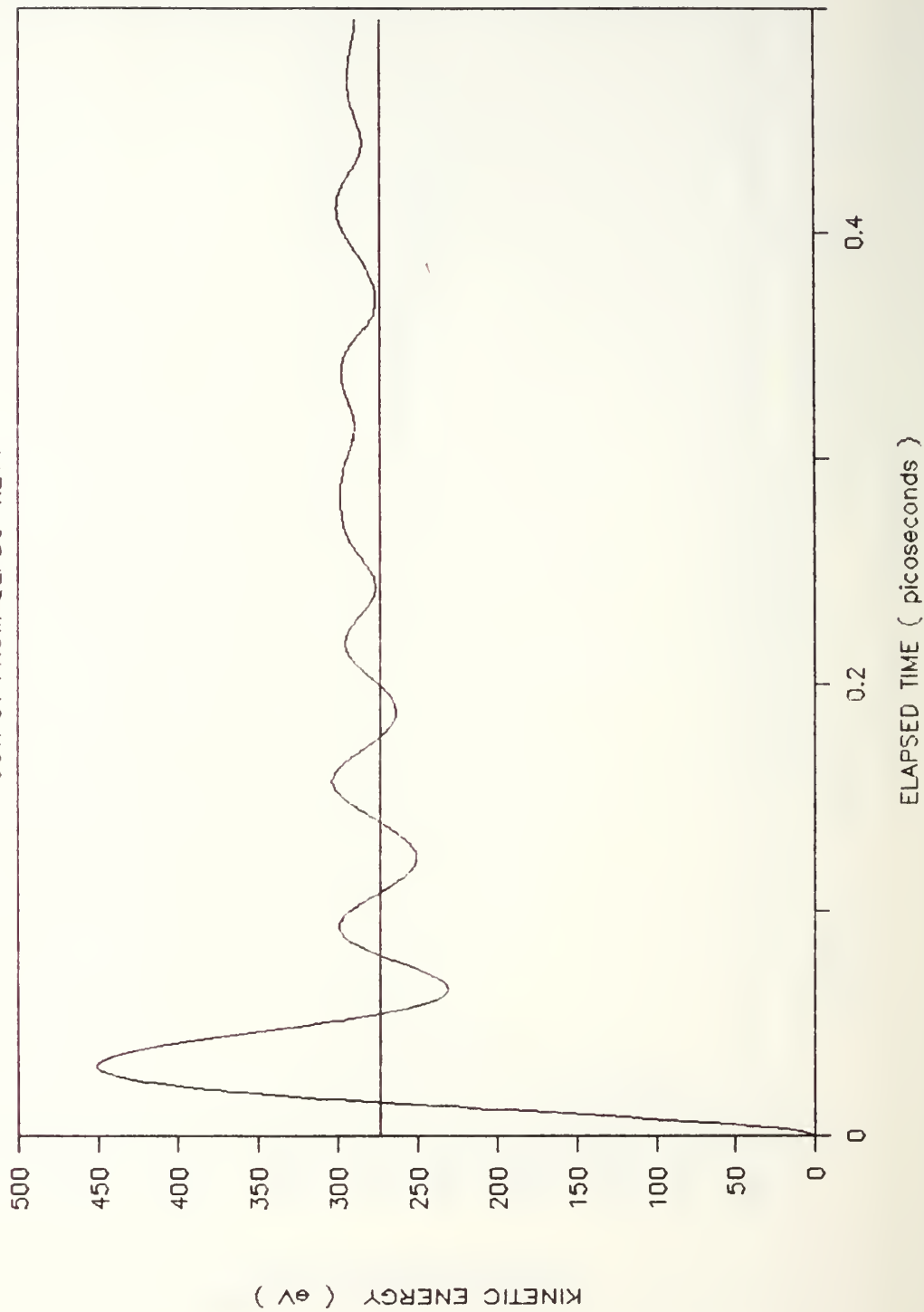
Figure 12. Kinetic Energy Versus Elapsed Time, QLPBC–REV1 Output.
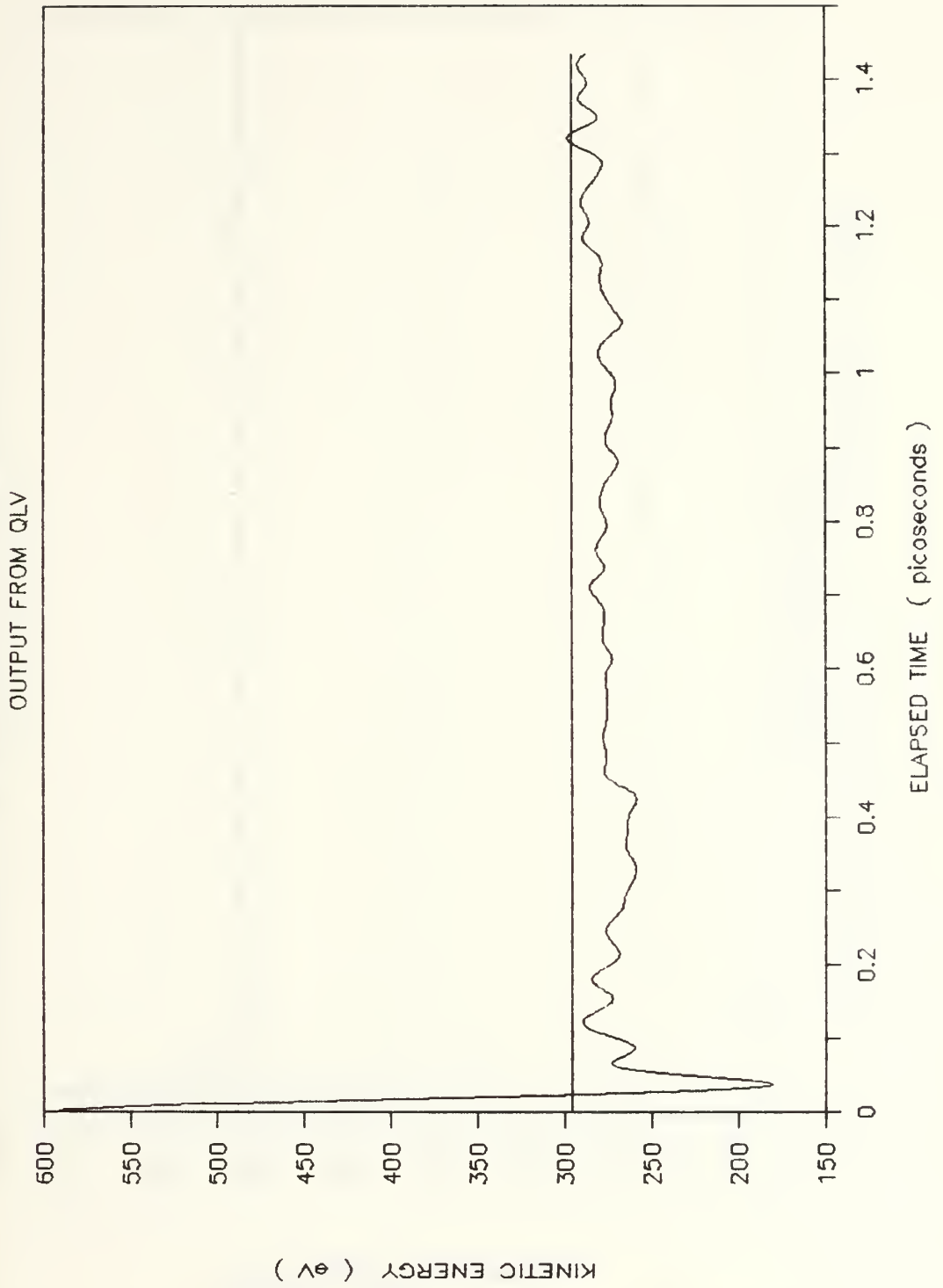
Figure 13. Kinetic Energy Versus Elapsed Time, QLV Output.

53
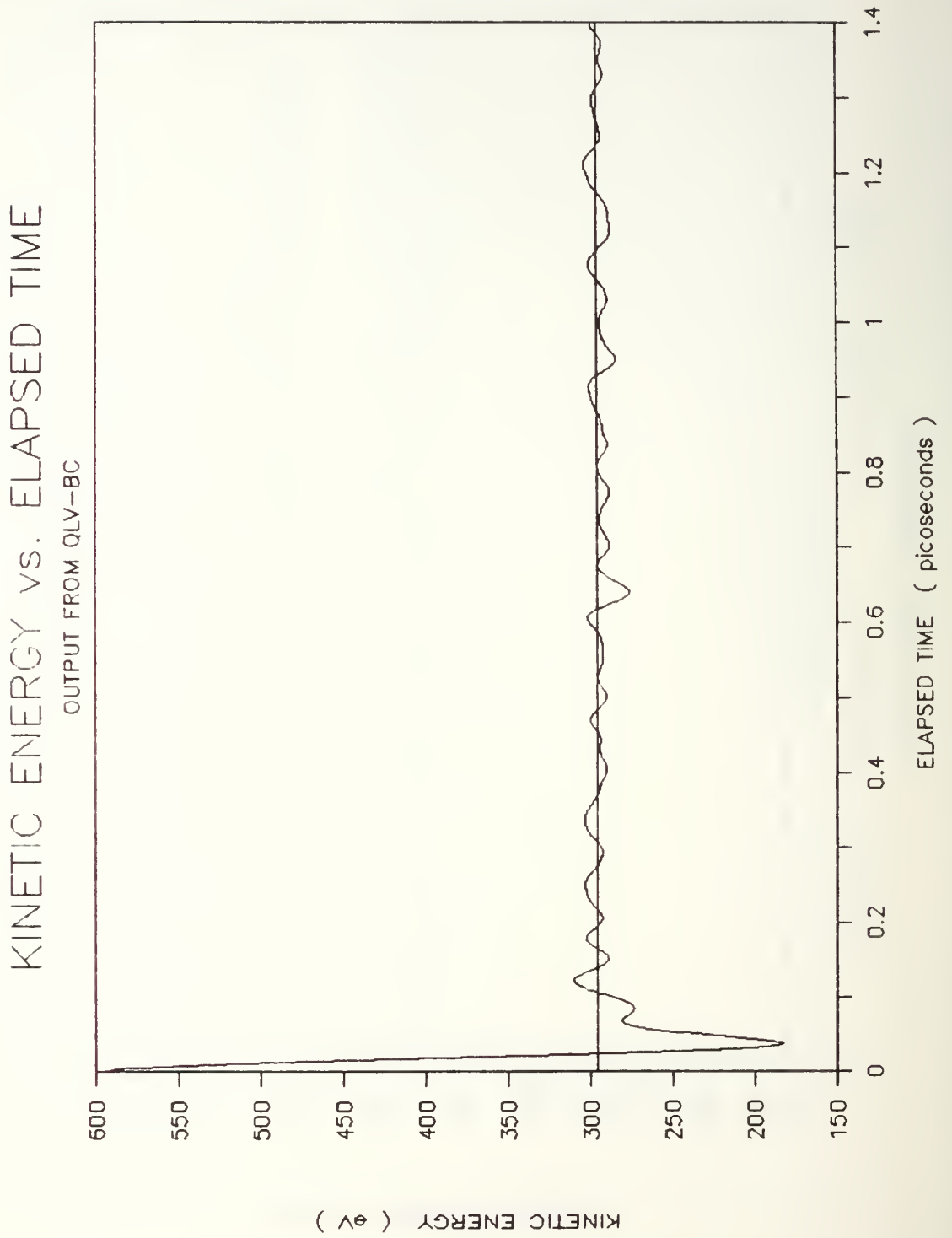
Figure 14. Kinetic Energy Versus Elapsed Time, QLVBC Output.

54
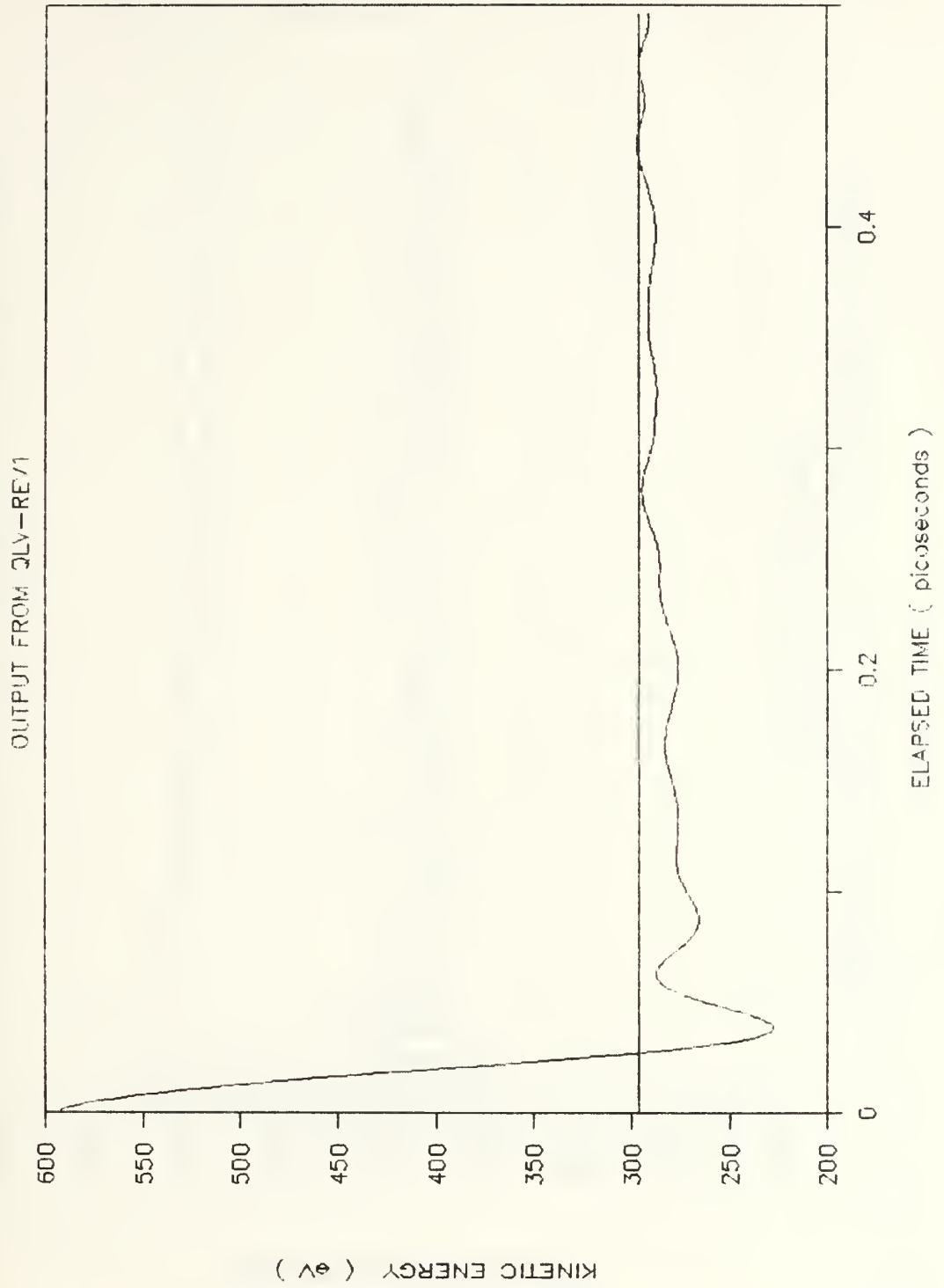
Figure 15. Kinetic Energy Versus Elapsed Time, QLV–REV1 Output.

55
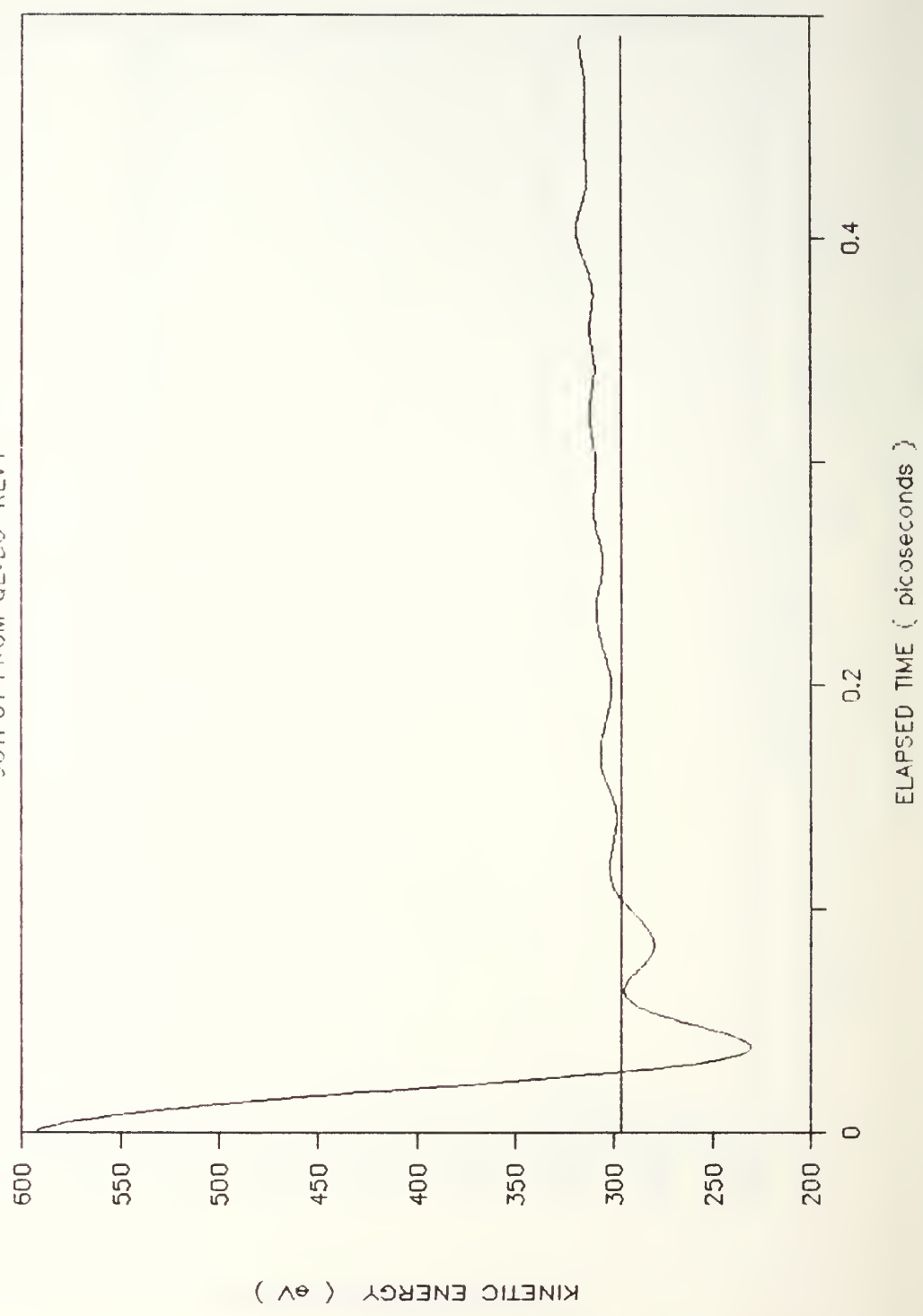
Figure 16. Kinetic Energy Versus Elapsed Time, QLVBC–REV1 Output.
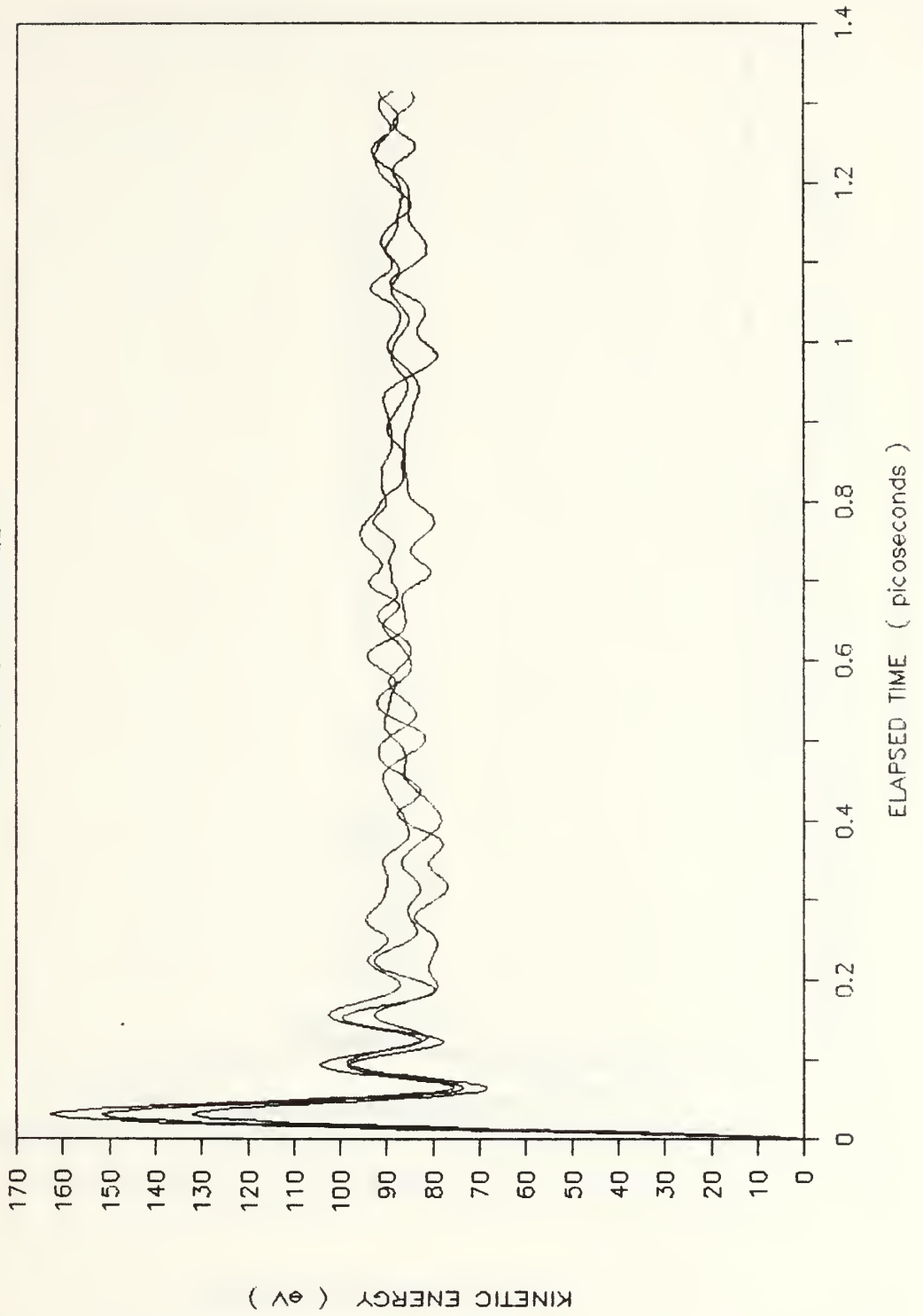
Figure 17. Components of KE Versus Elapsed Time, QLP Output.
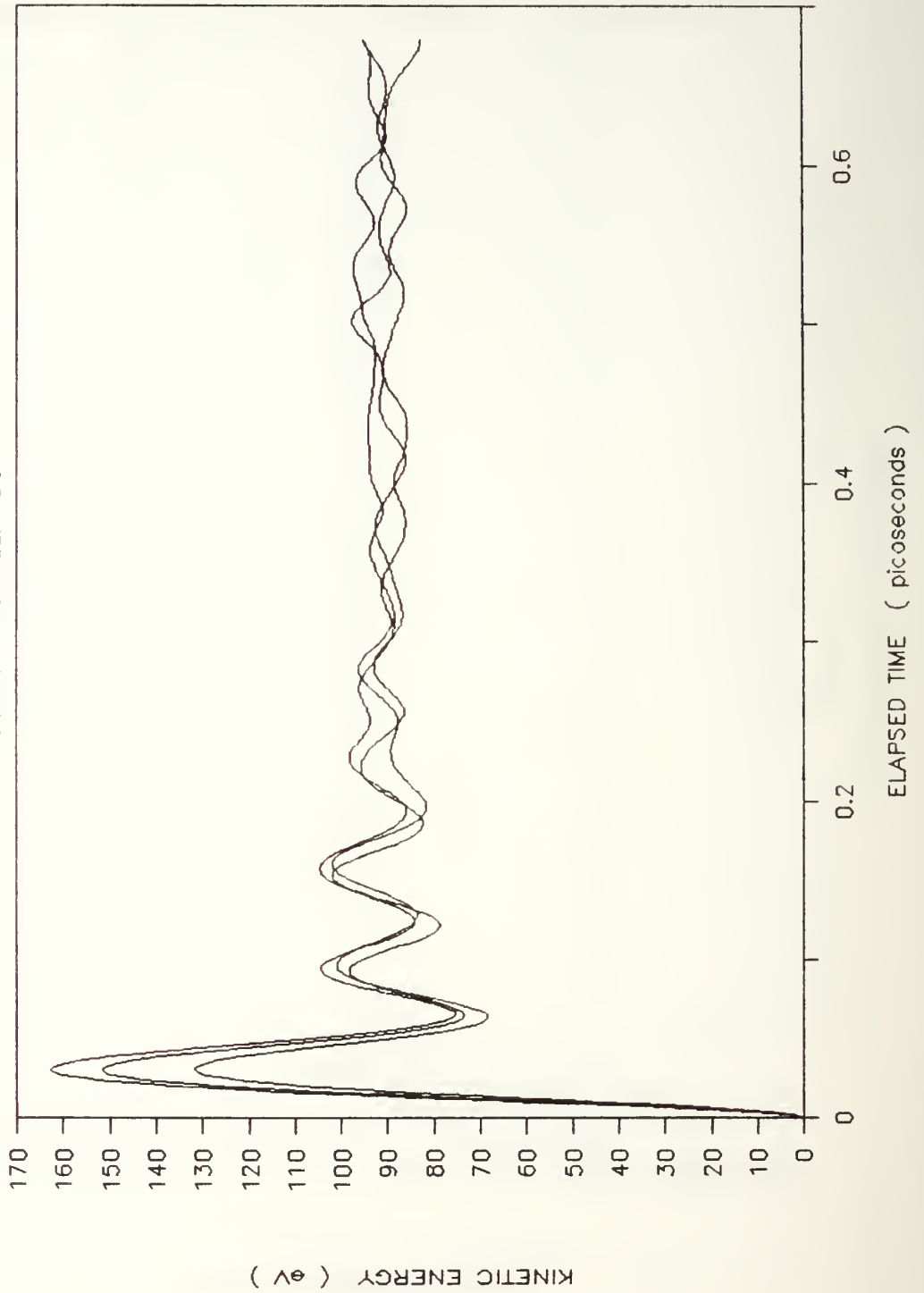
Figure 18. Components of KE Versus Elapsed Time, QLPBC Output.

58
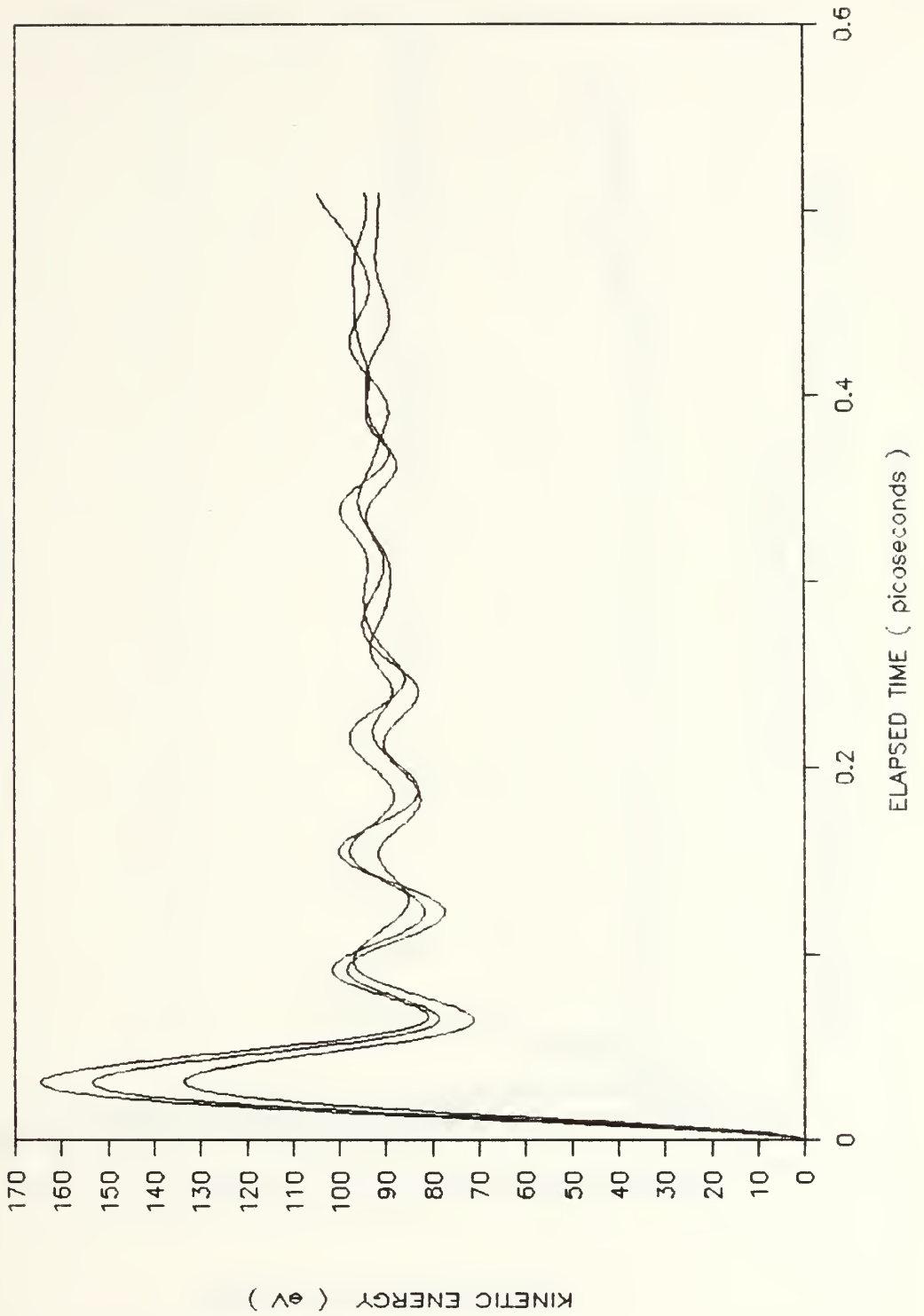
Figure 19. Components of KE Versus Elapsed Time, QLP–REV1 Output.

59
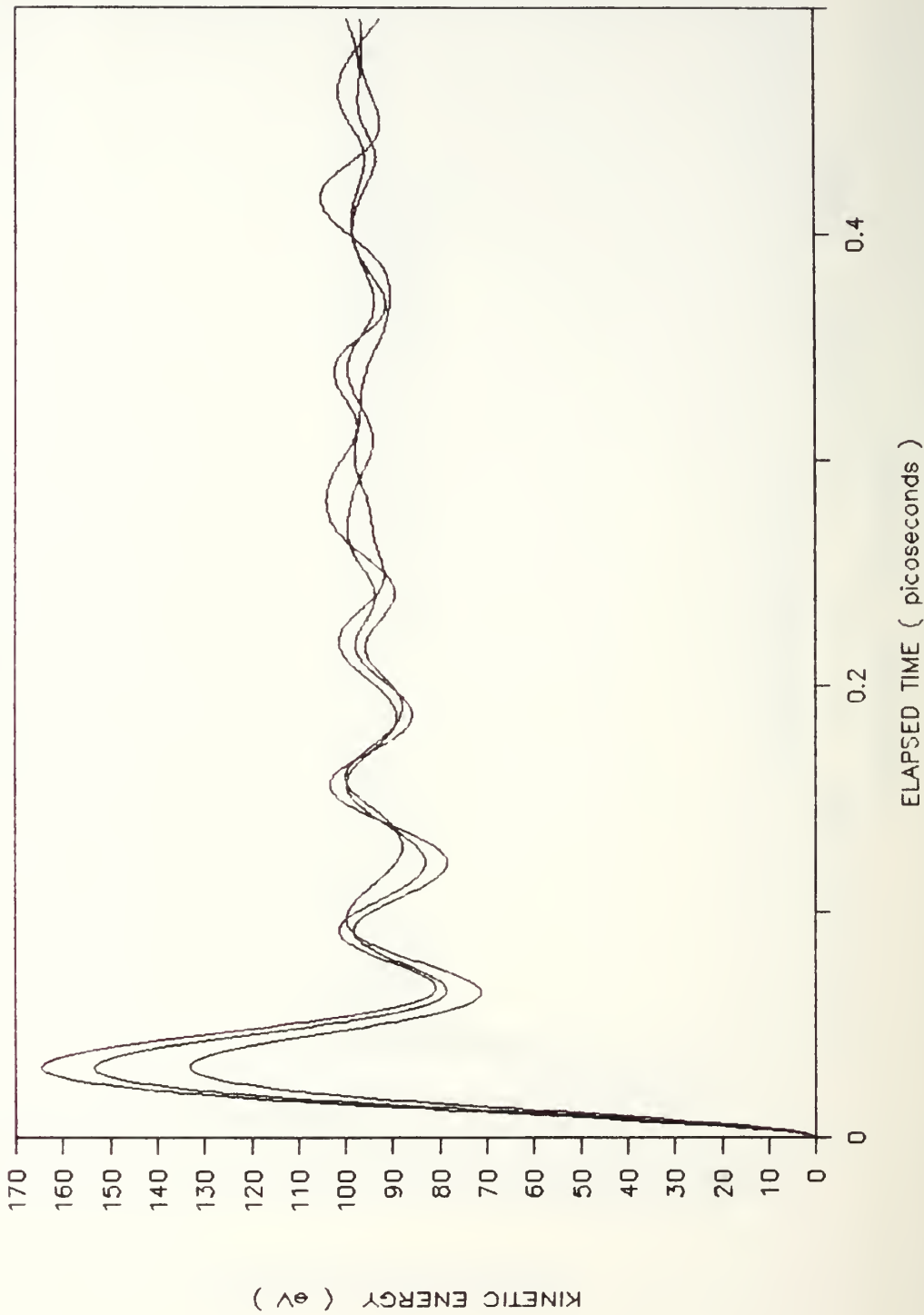
Figure 20. Components of KE Versus Elapsed Time, QLPBC–REV1 Output.
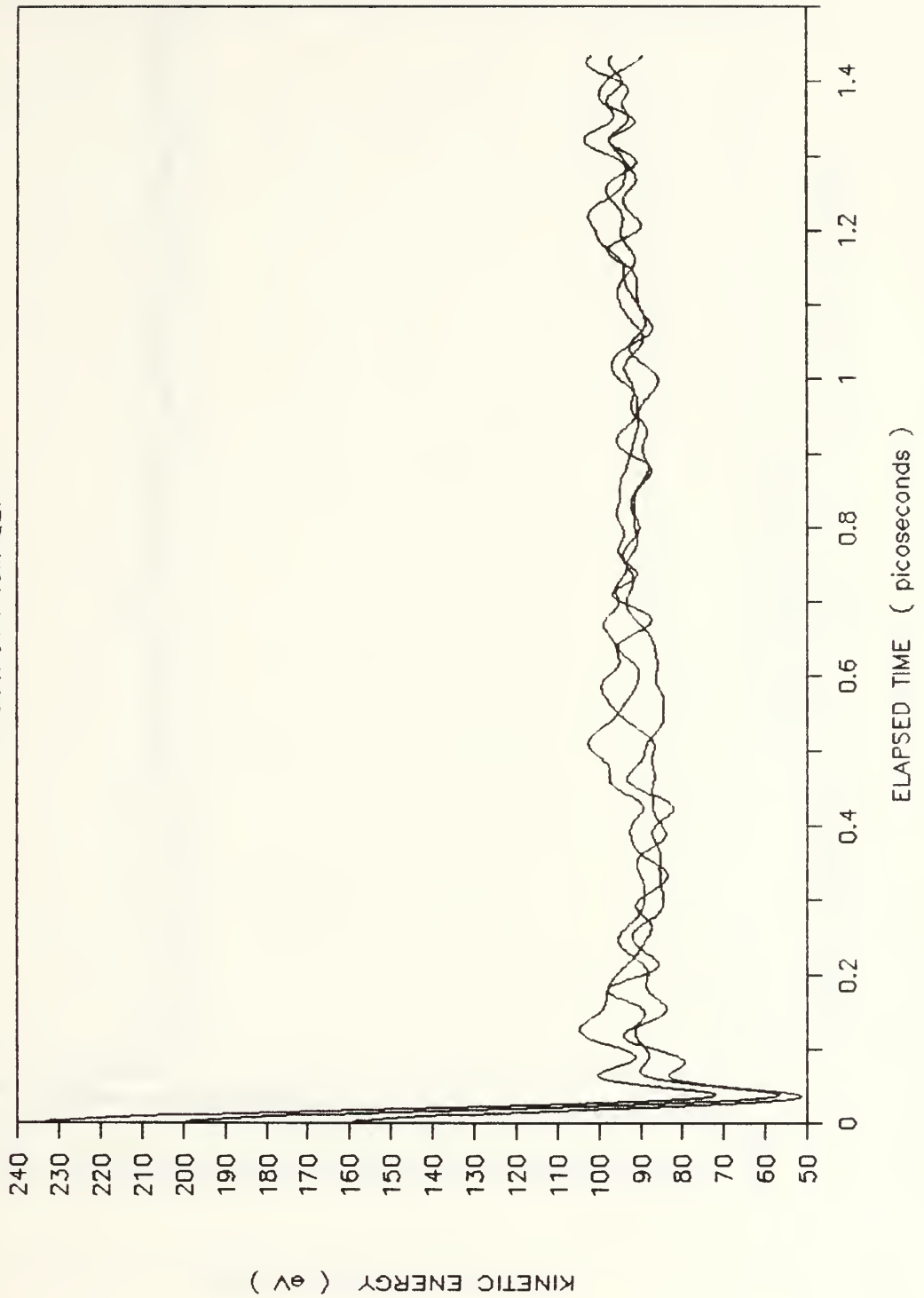
Figure 21. Components of KE Versus Elapsed Time, QLV Output.

61
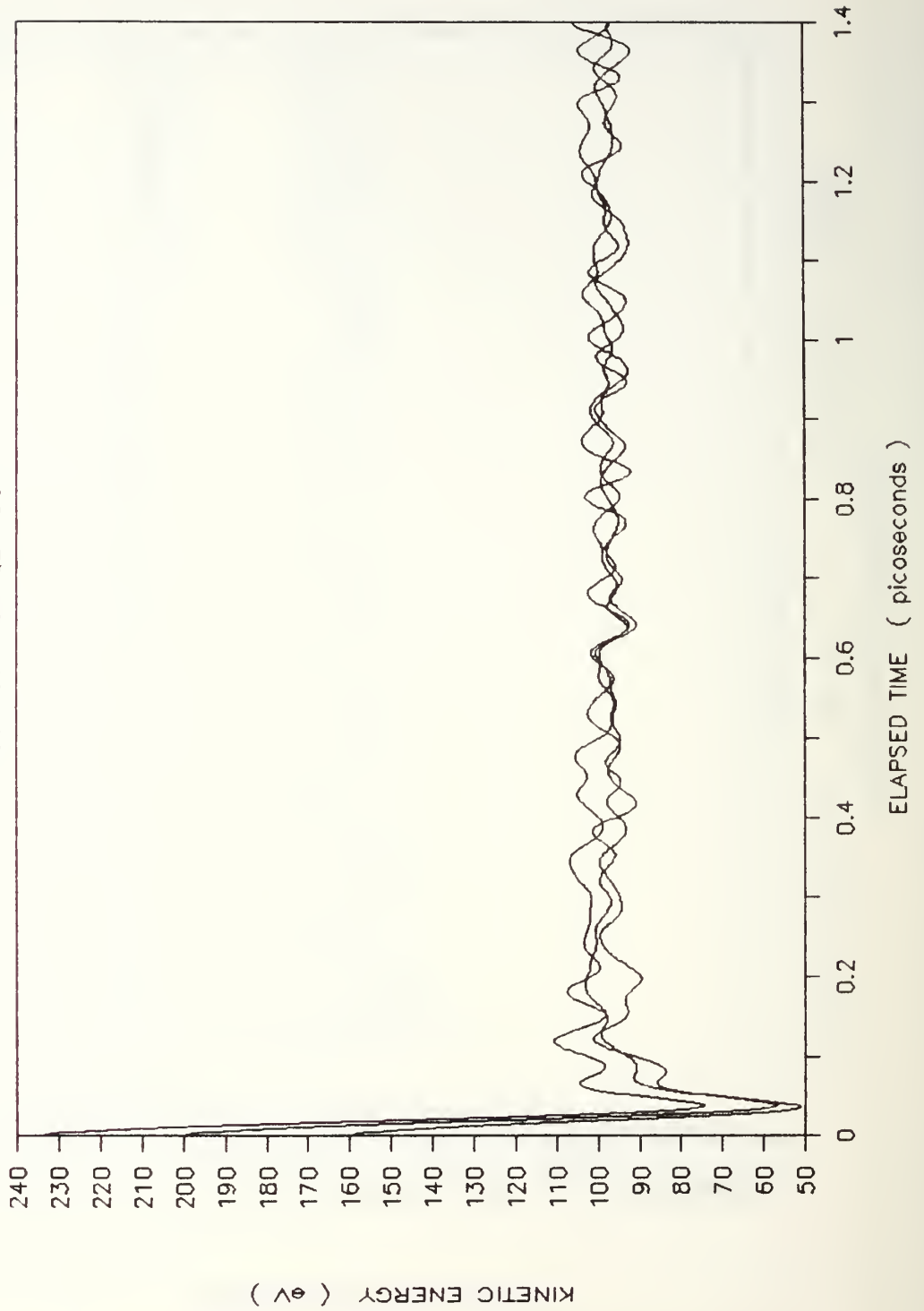
Figure 22. Components of KE Versus Elapsed Time, QLVBC Output.

62
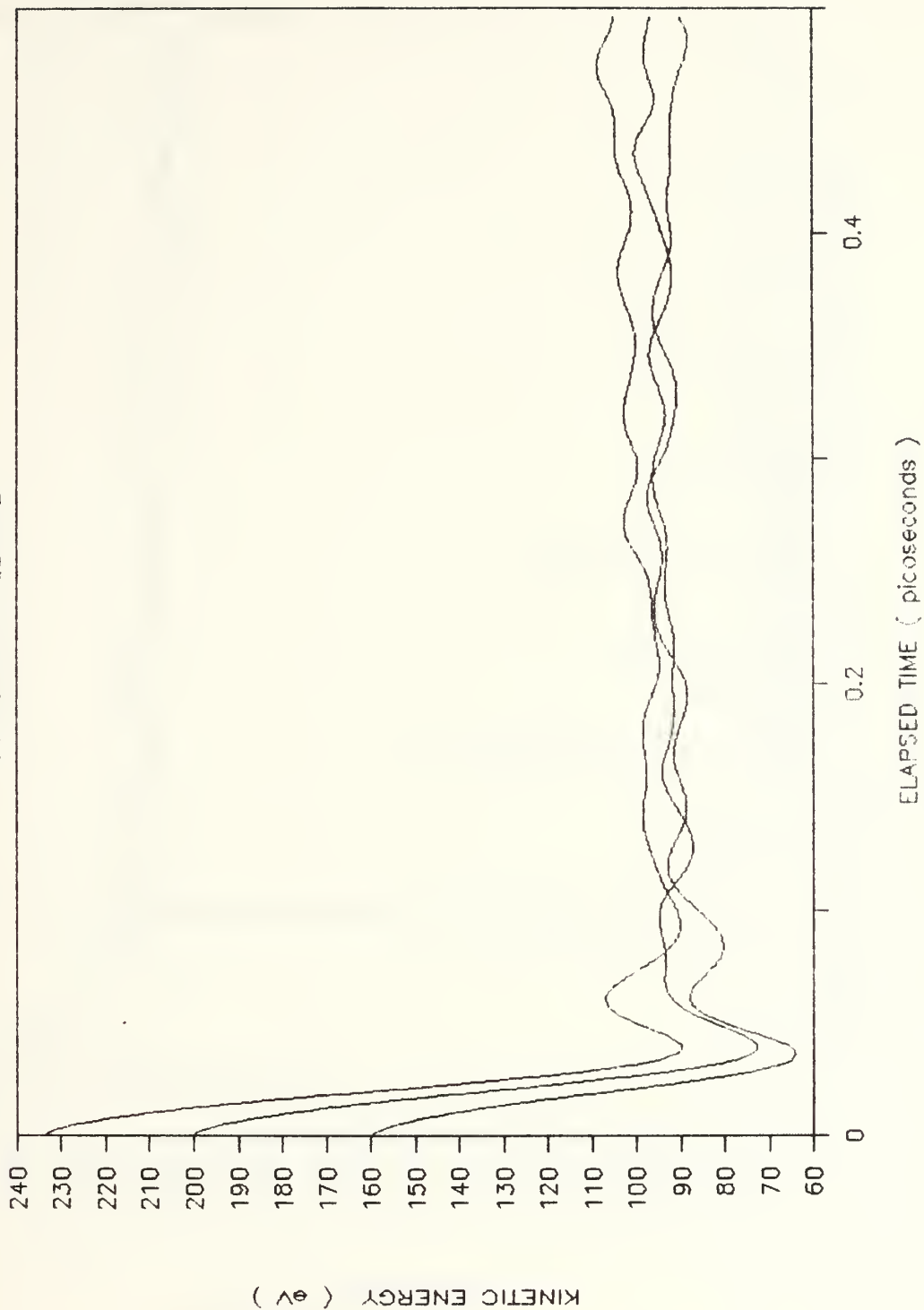
Figure 23. Components of KE Versus Elapsed Time, QLV–REV1 Output.

63
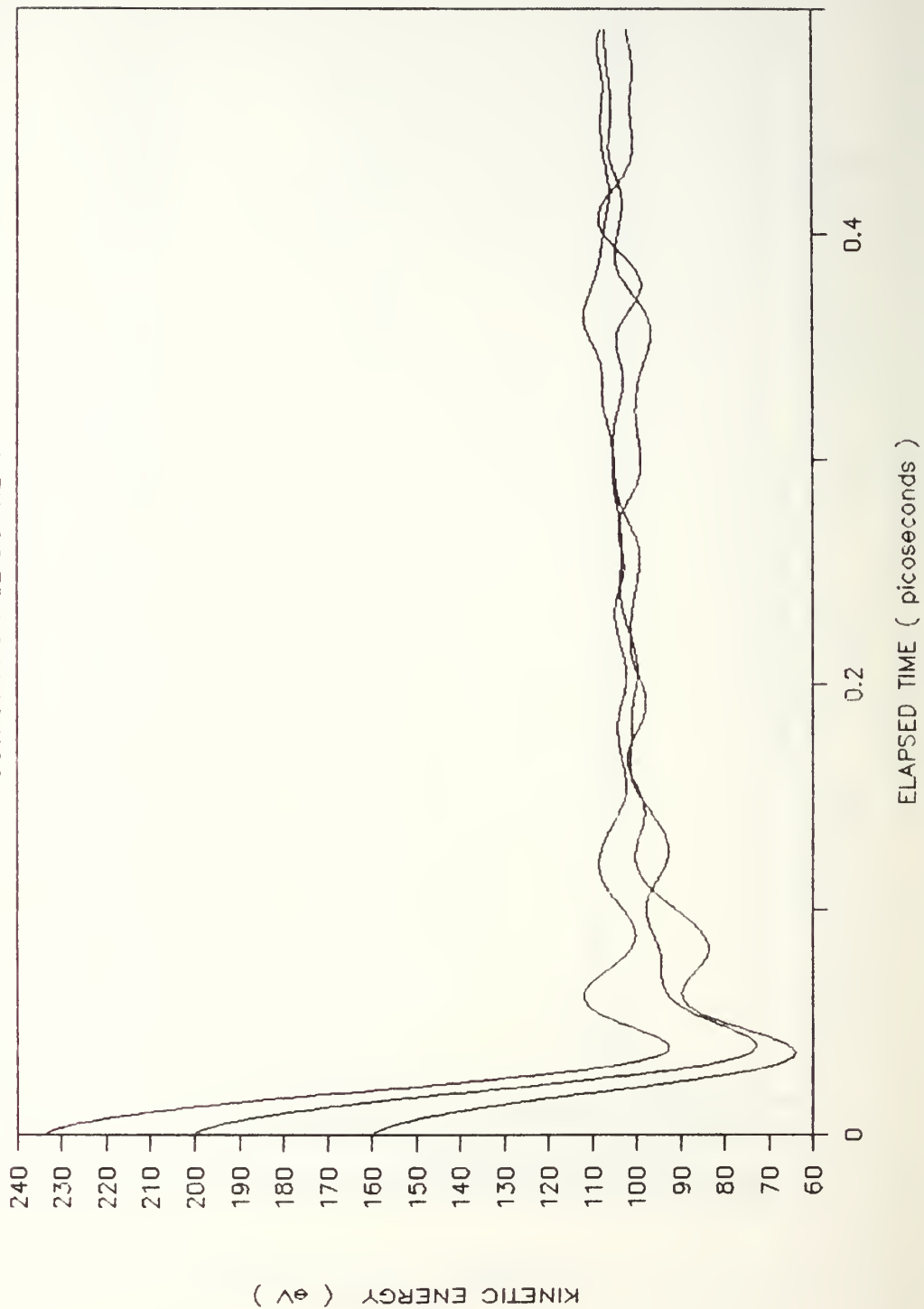
Figure 24. Components of KE Versus Elapsed Time, QLVBC—REV1 Output.

64

Figure 25. Radial Distribution, Unwarmed Crystal.
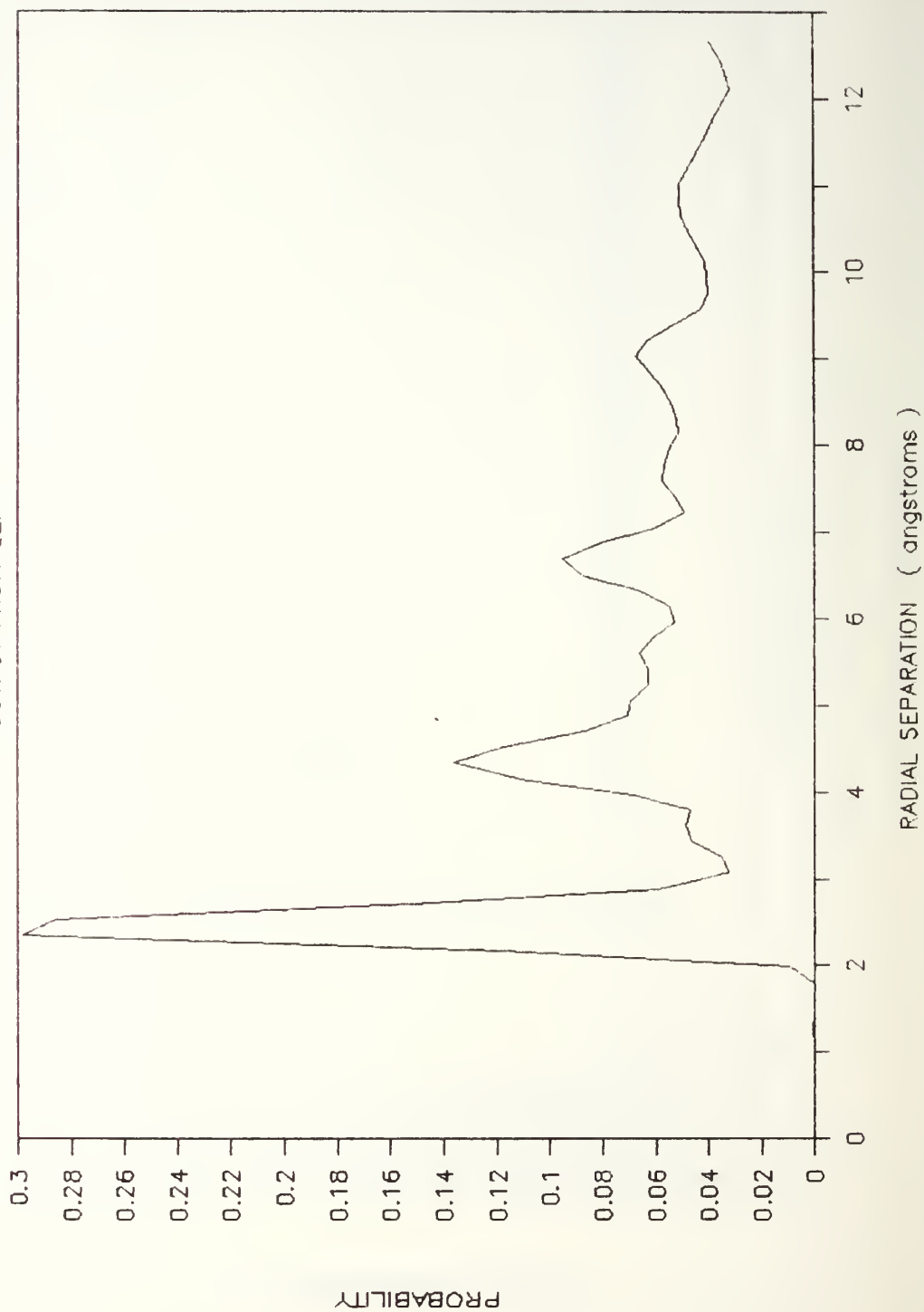
Figure 26. Radial Distribution, QLP Output.

66
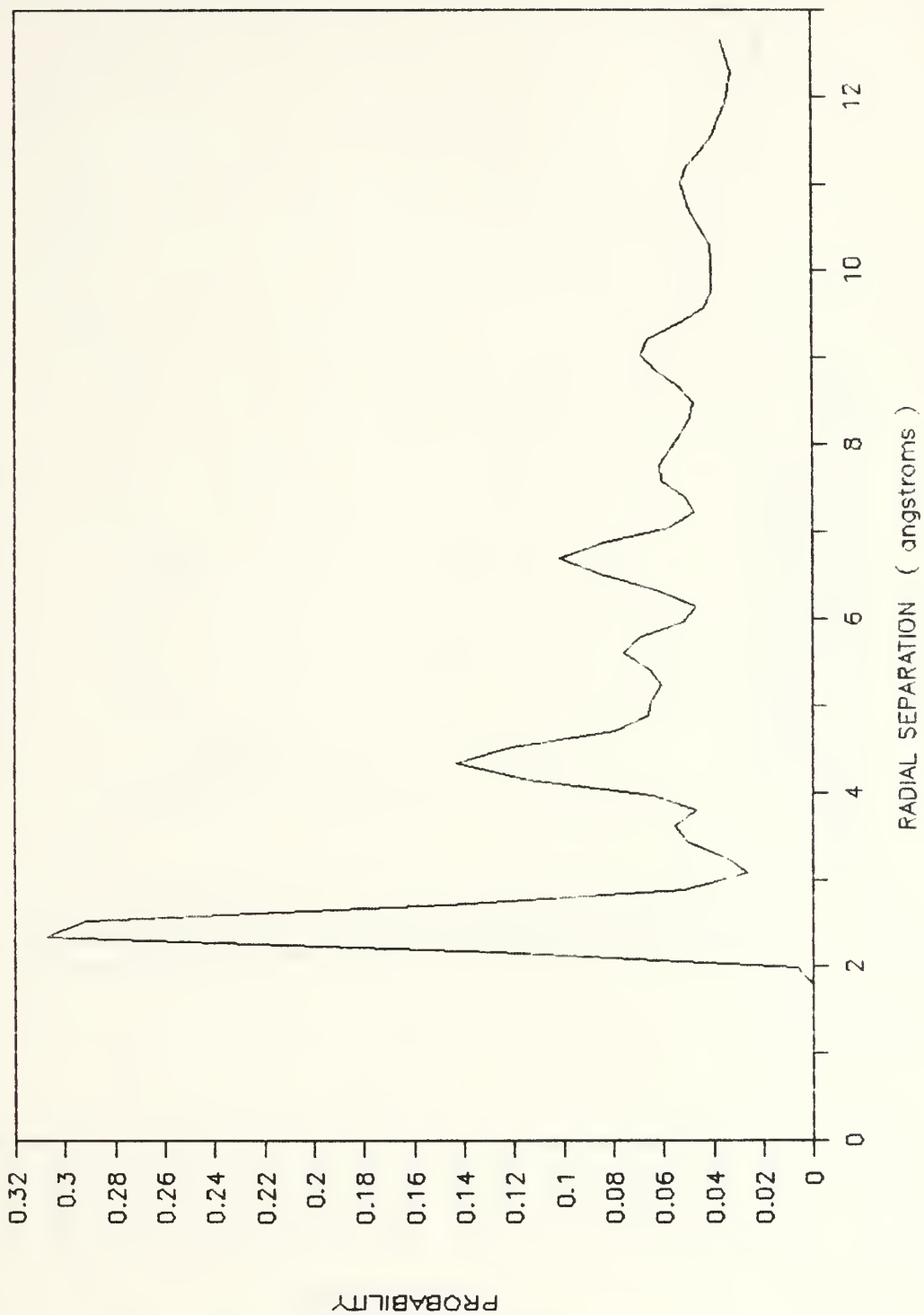
Figure 27. Radial Distribution, QLPBC Output.

67
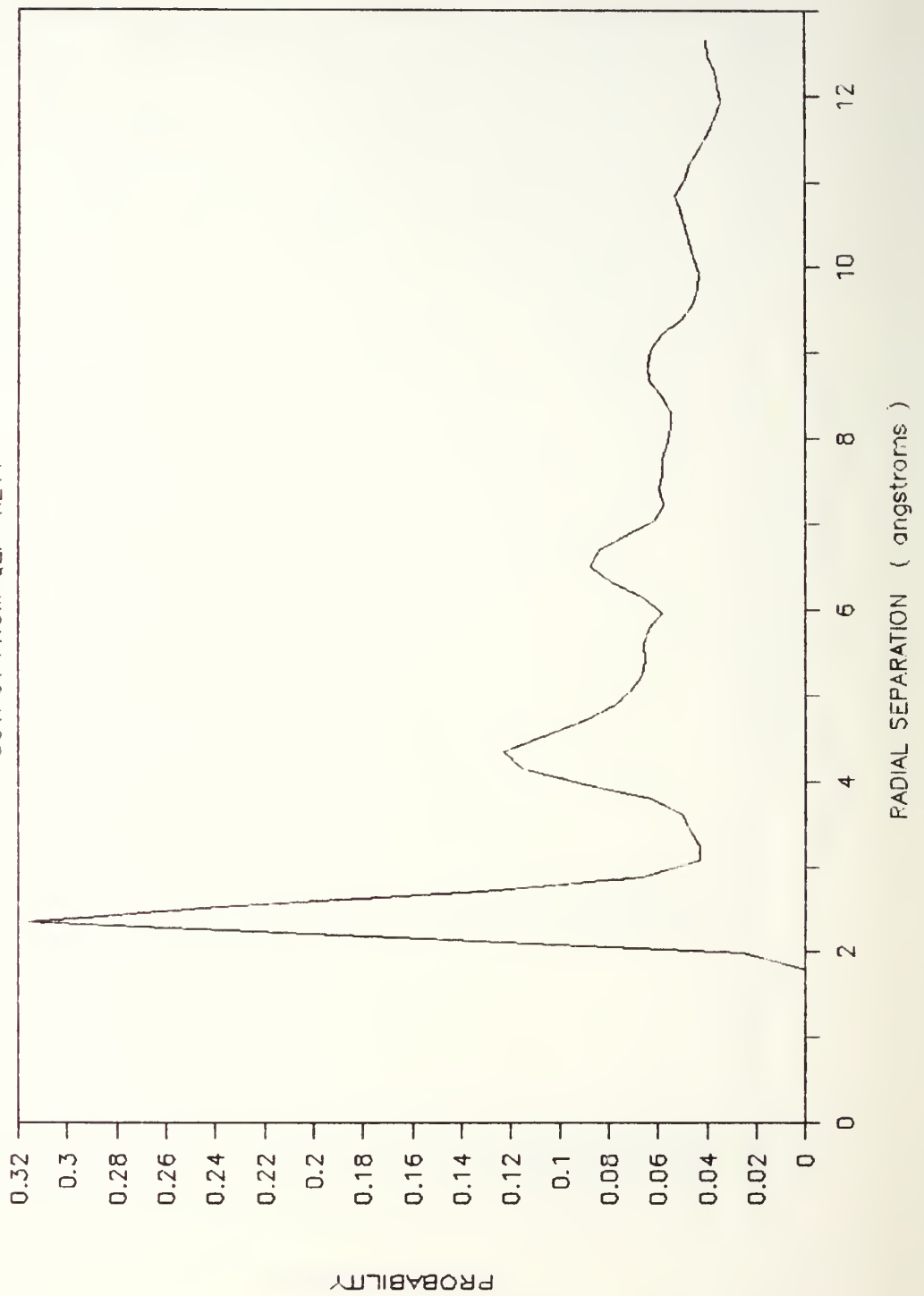
Figure 28. Radial Distribution, QLP–REV1 Output.

68
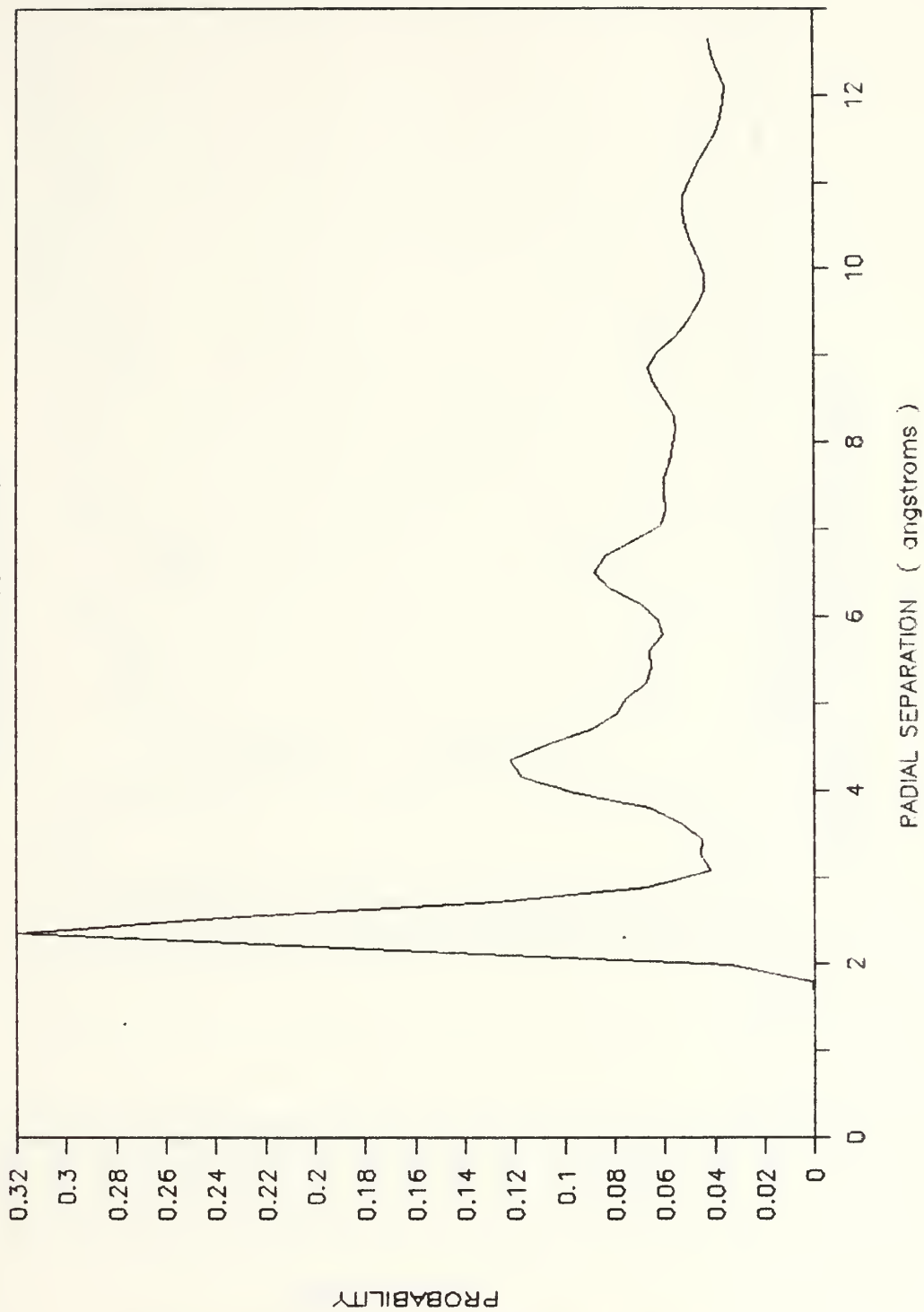
Figure 29. Radial Distribution, QLPBC–REV1 Output.

69
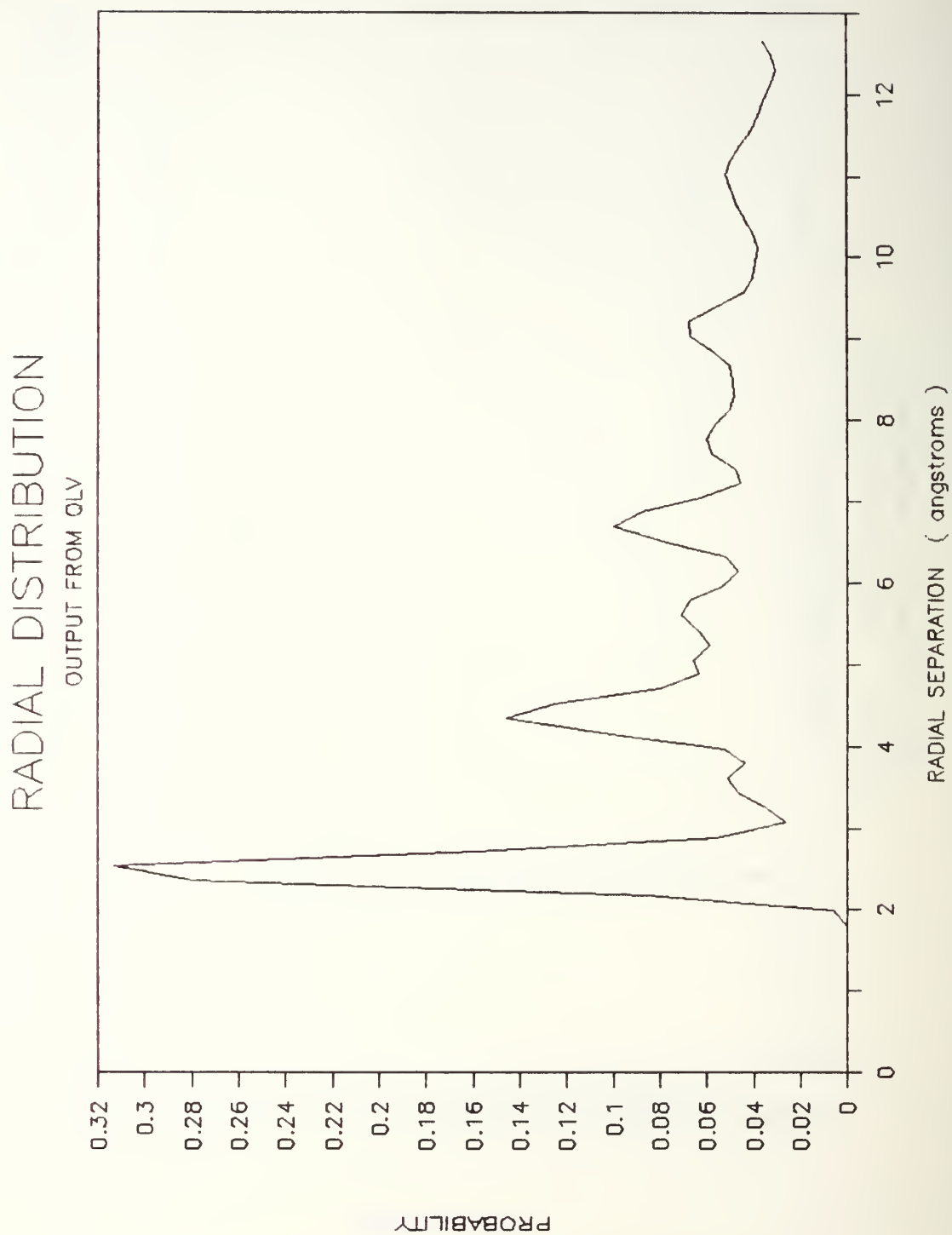
Figure 30. Radial Distribution, QLV Output.
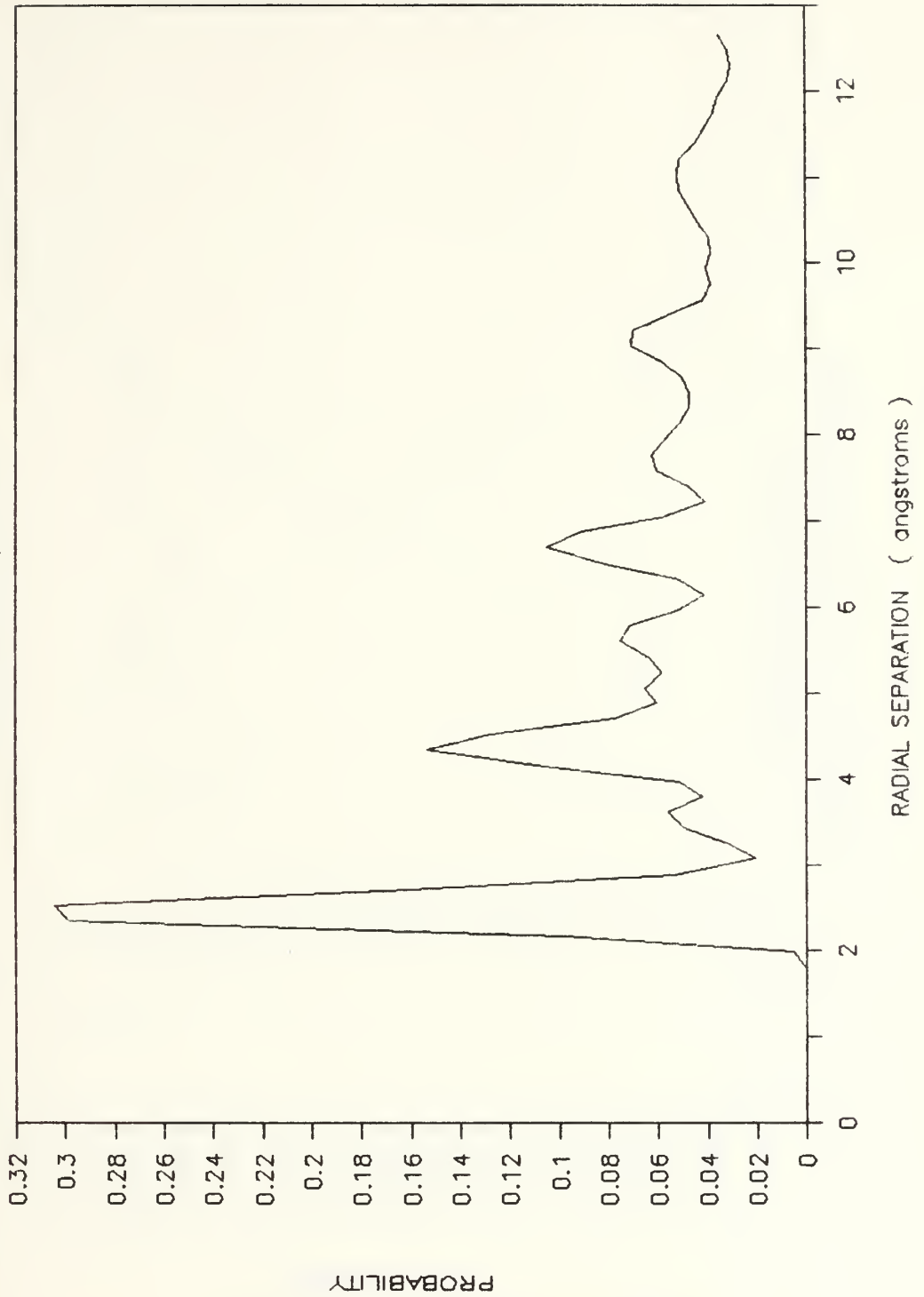
Figure 31. Radial Distribution, QLVBC Output.

71
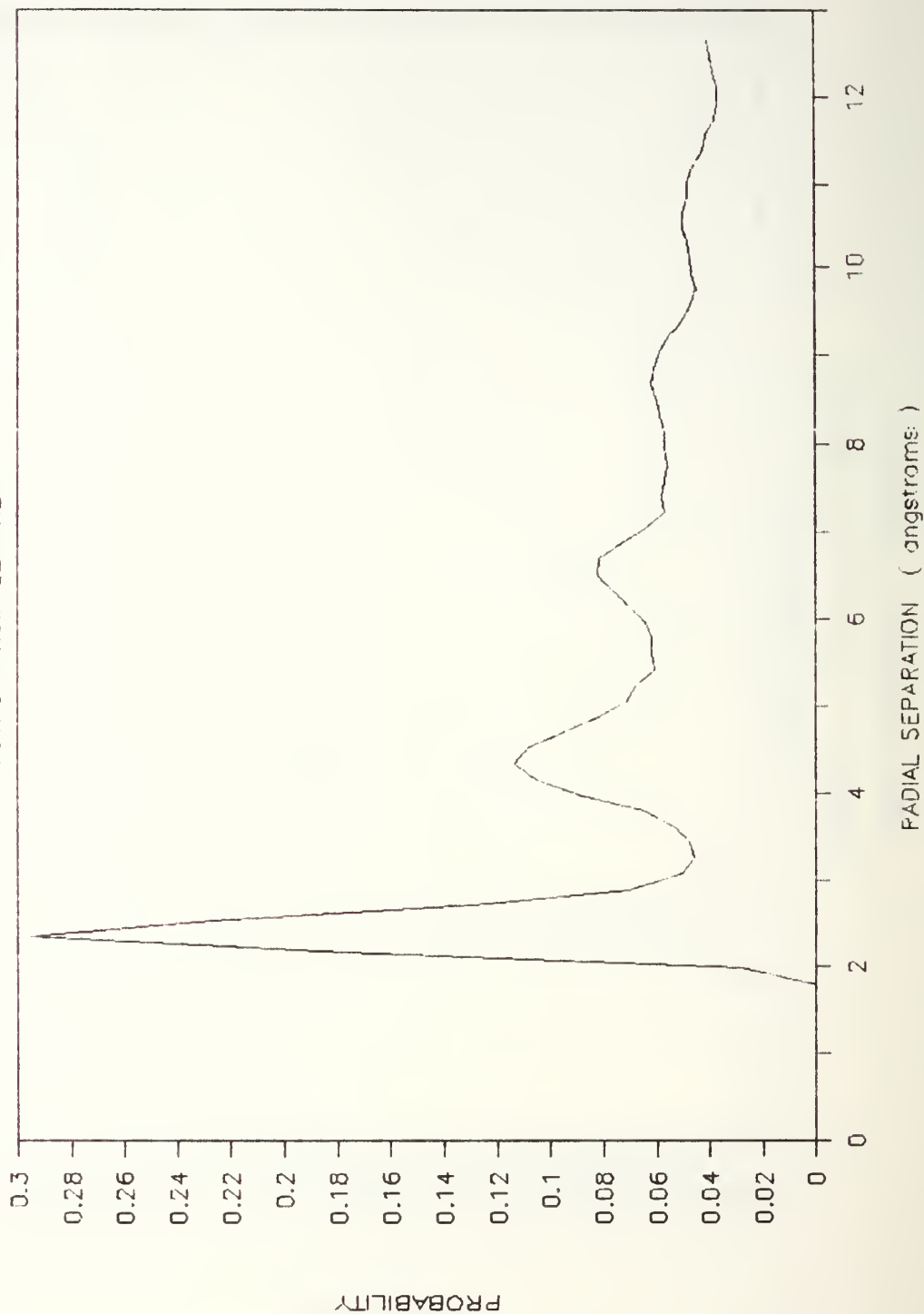
Figure 32. Radial Distribution, QLV–REV1 Output.
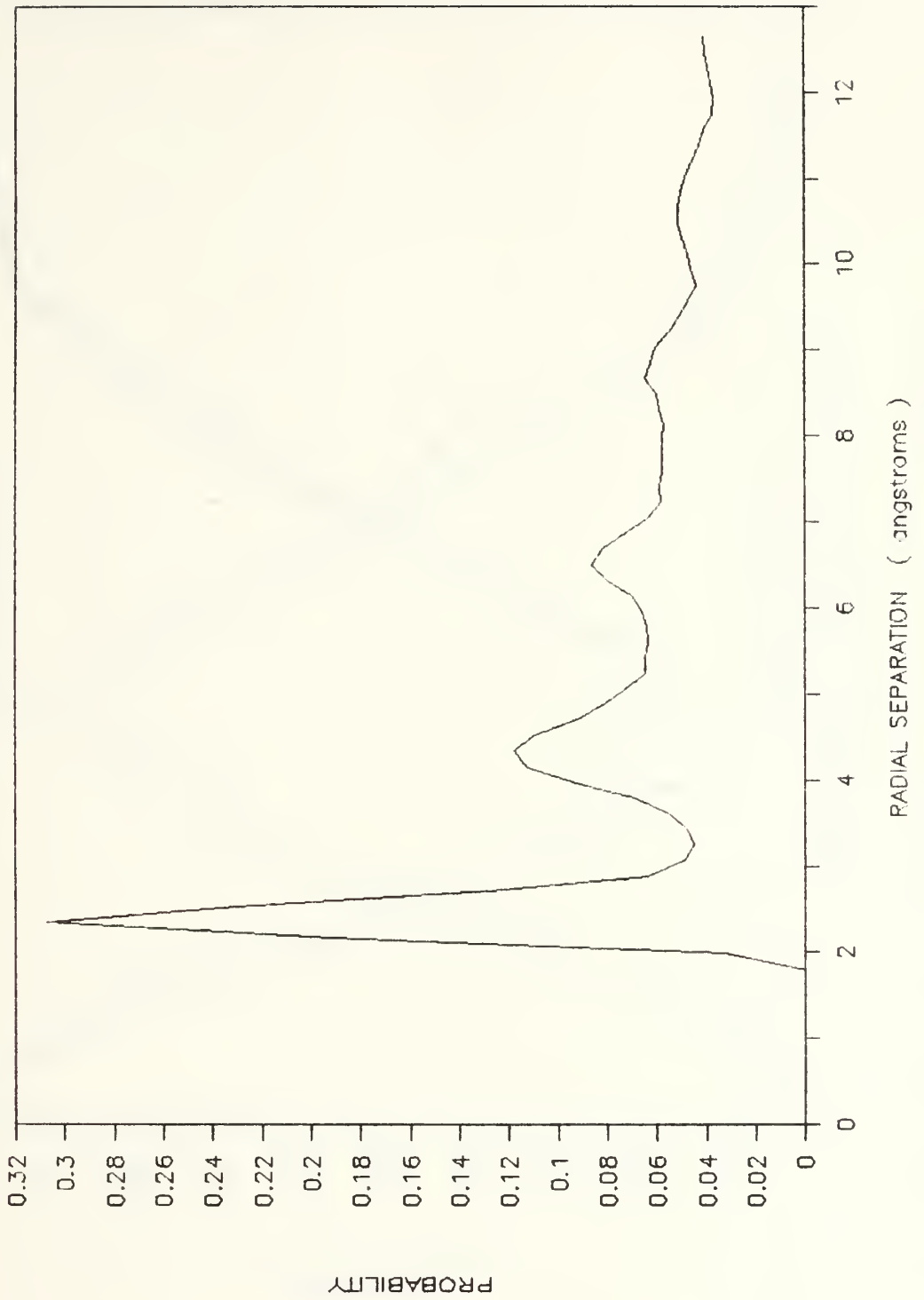
Figure 33. Radial Distribution, QLVBC–REV1 Output.

73
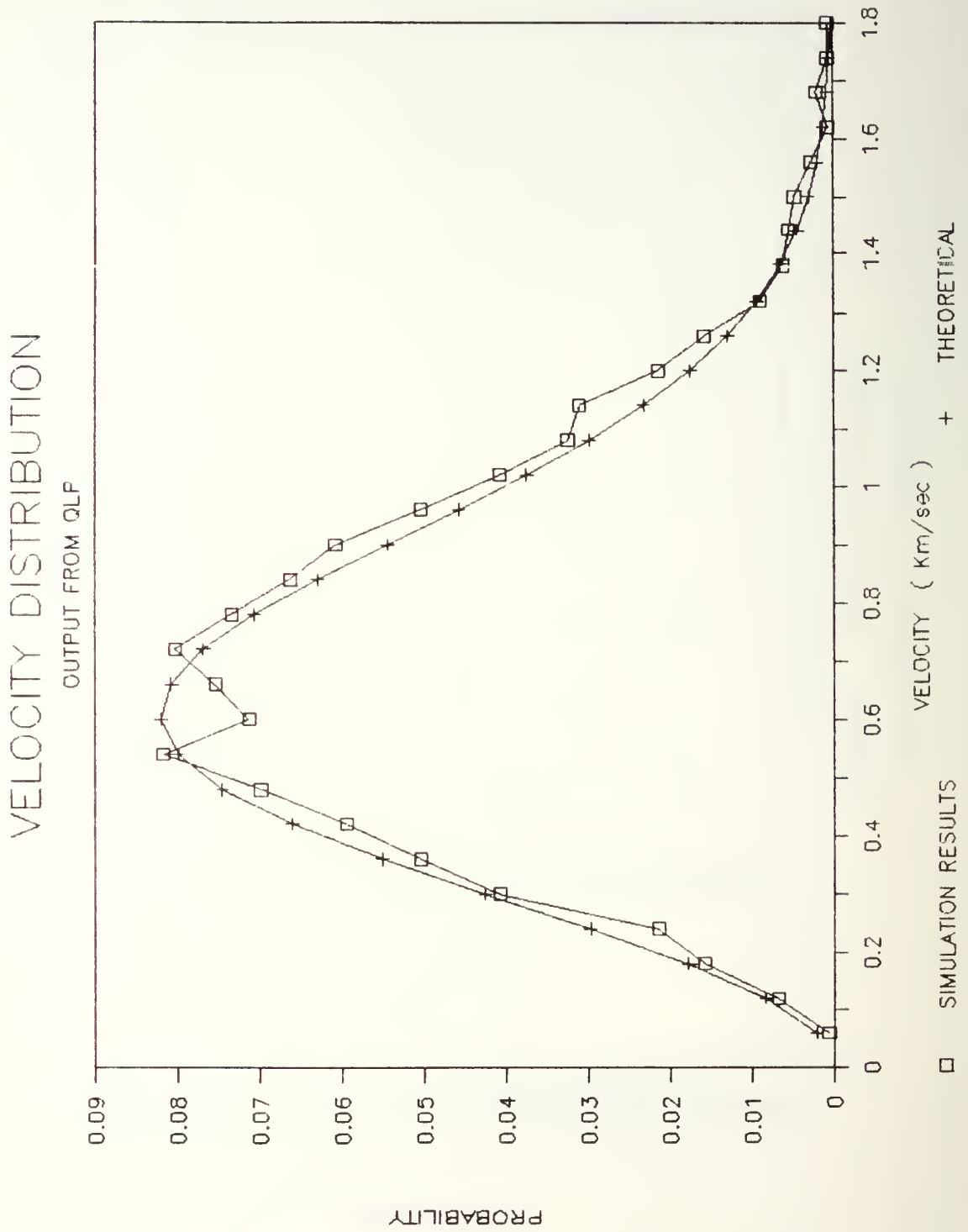
Figure 34. Velocity Distribution, QLP Output.
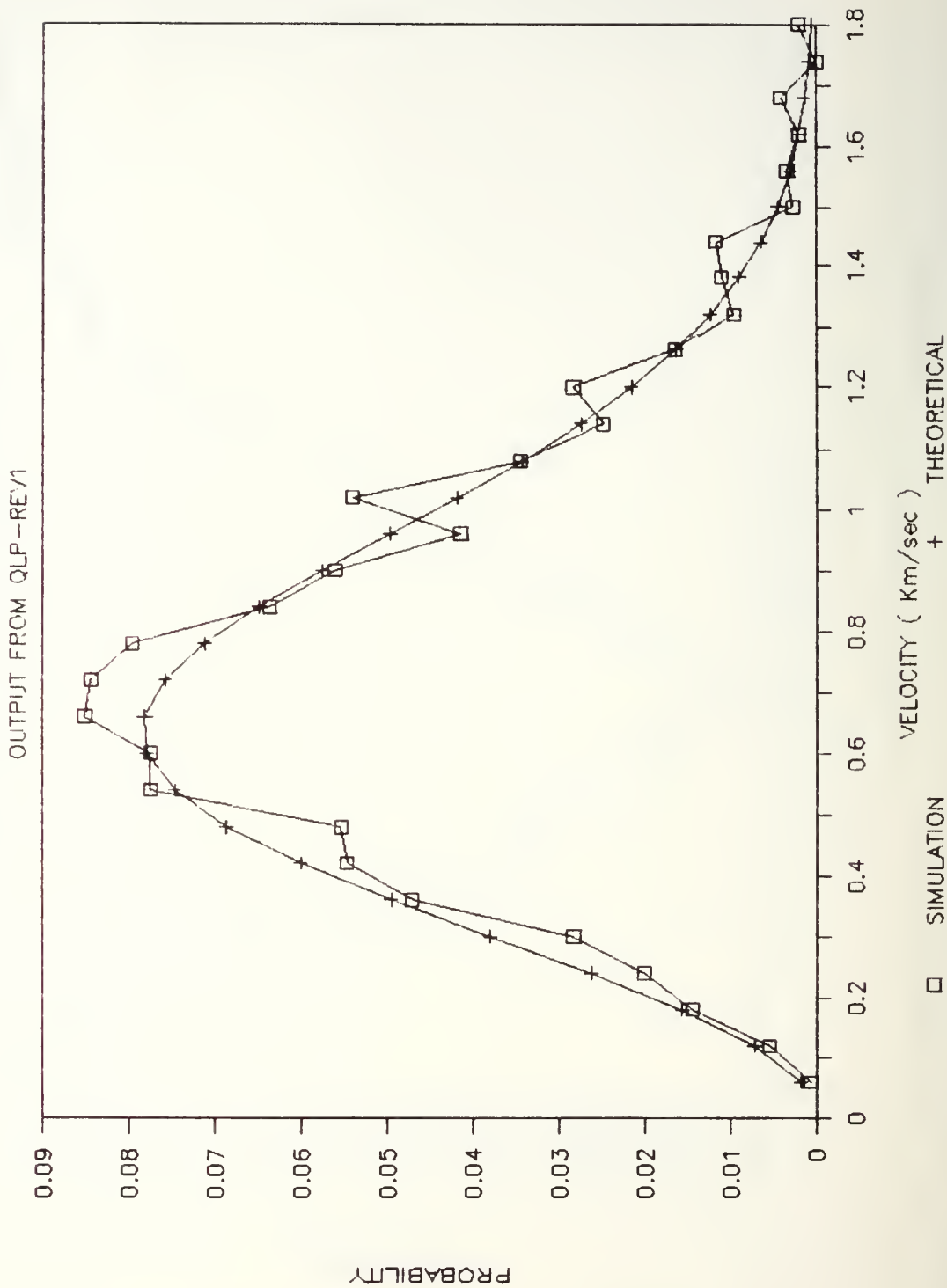
74
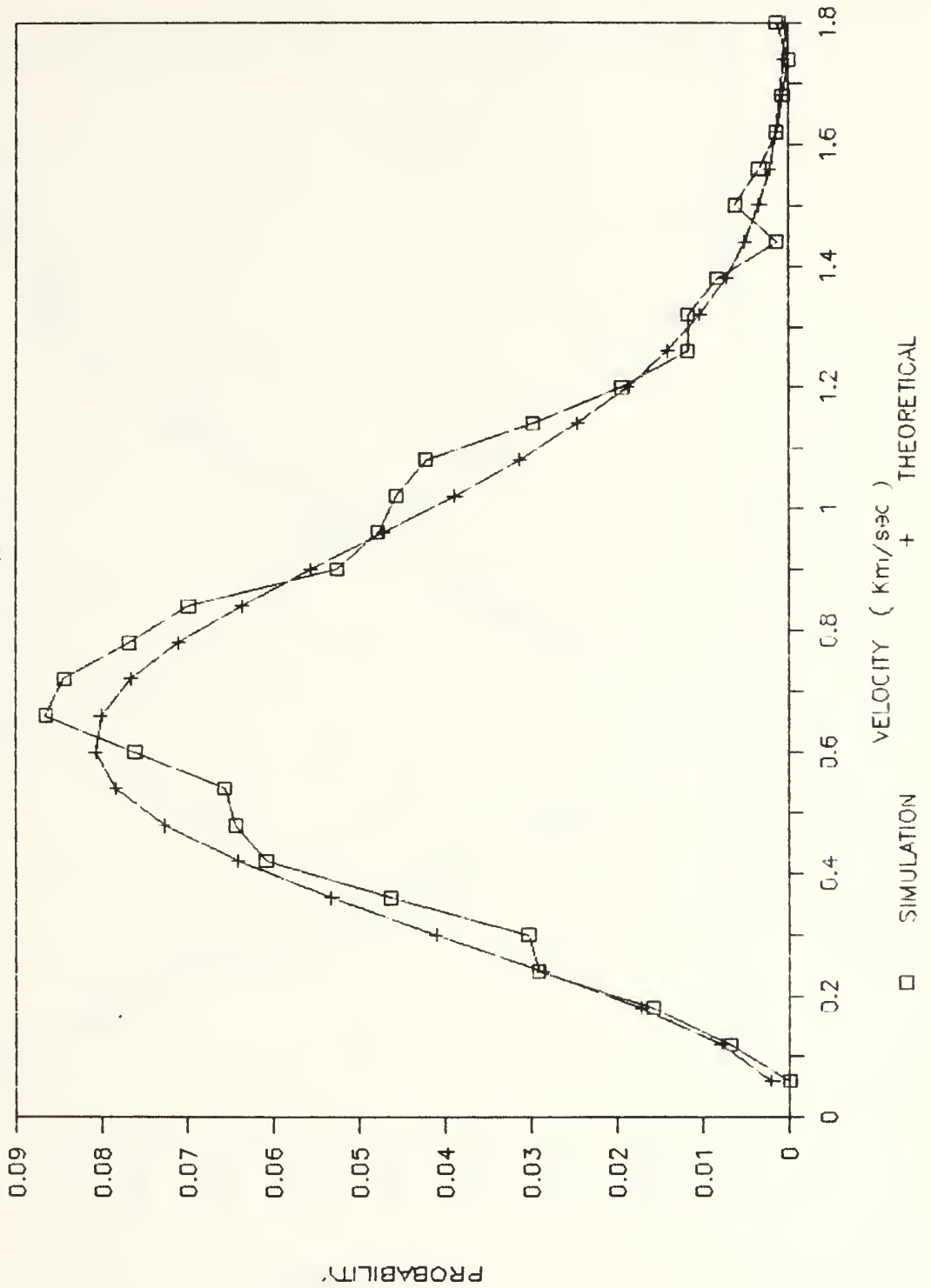
Figure 35. Velocity Distribution, QLPBC Output.

Figure 36. Velocity Distribution, QLP–REV1 Output.
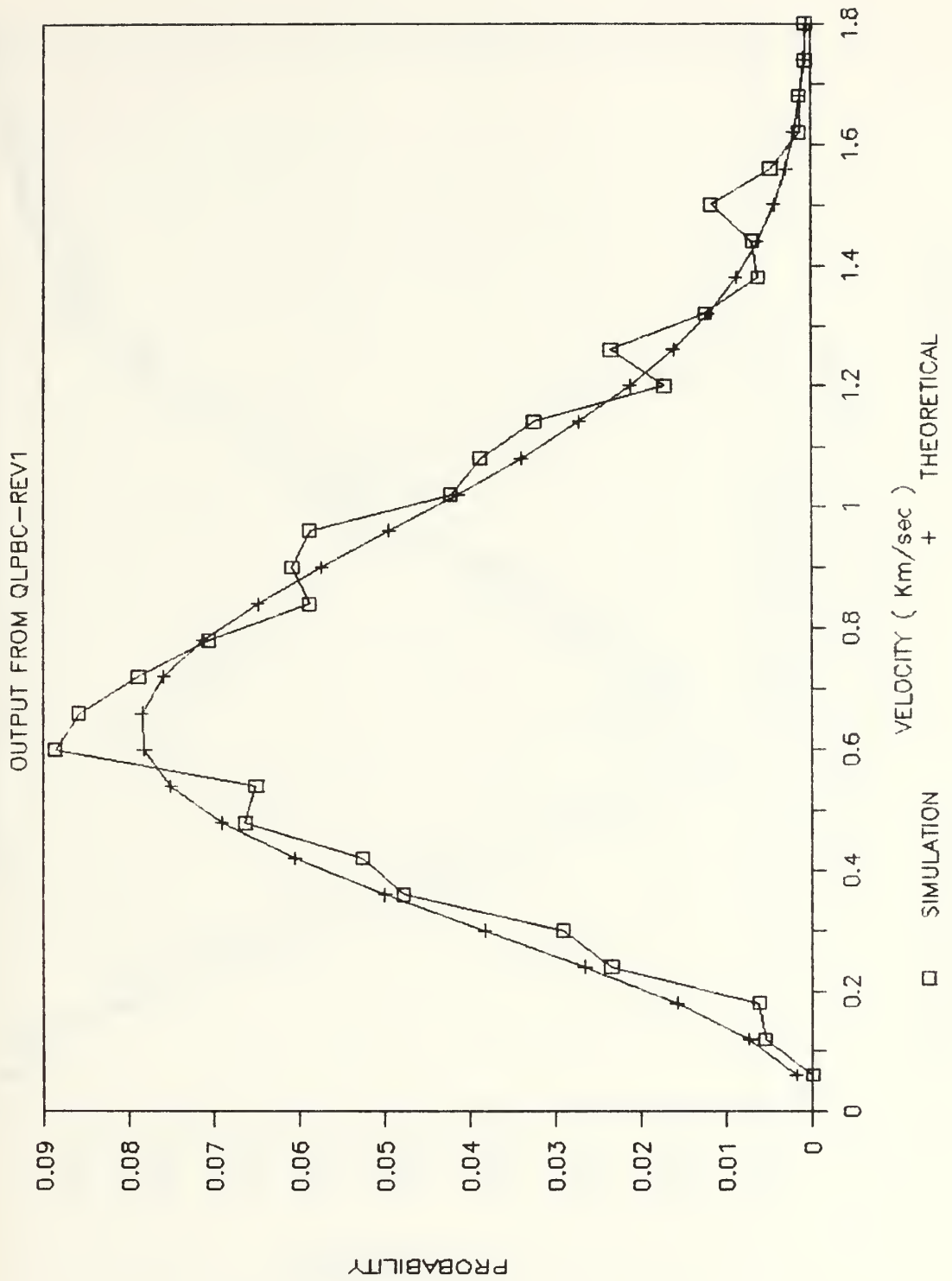
Figure 37. Velocity Distribution, QLPBC–REV1 Output.
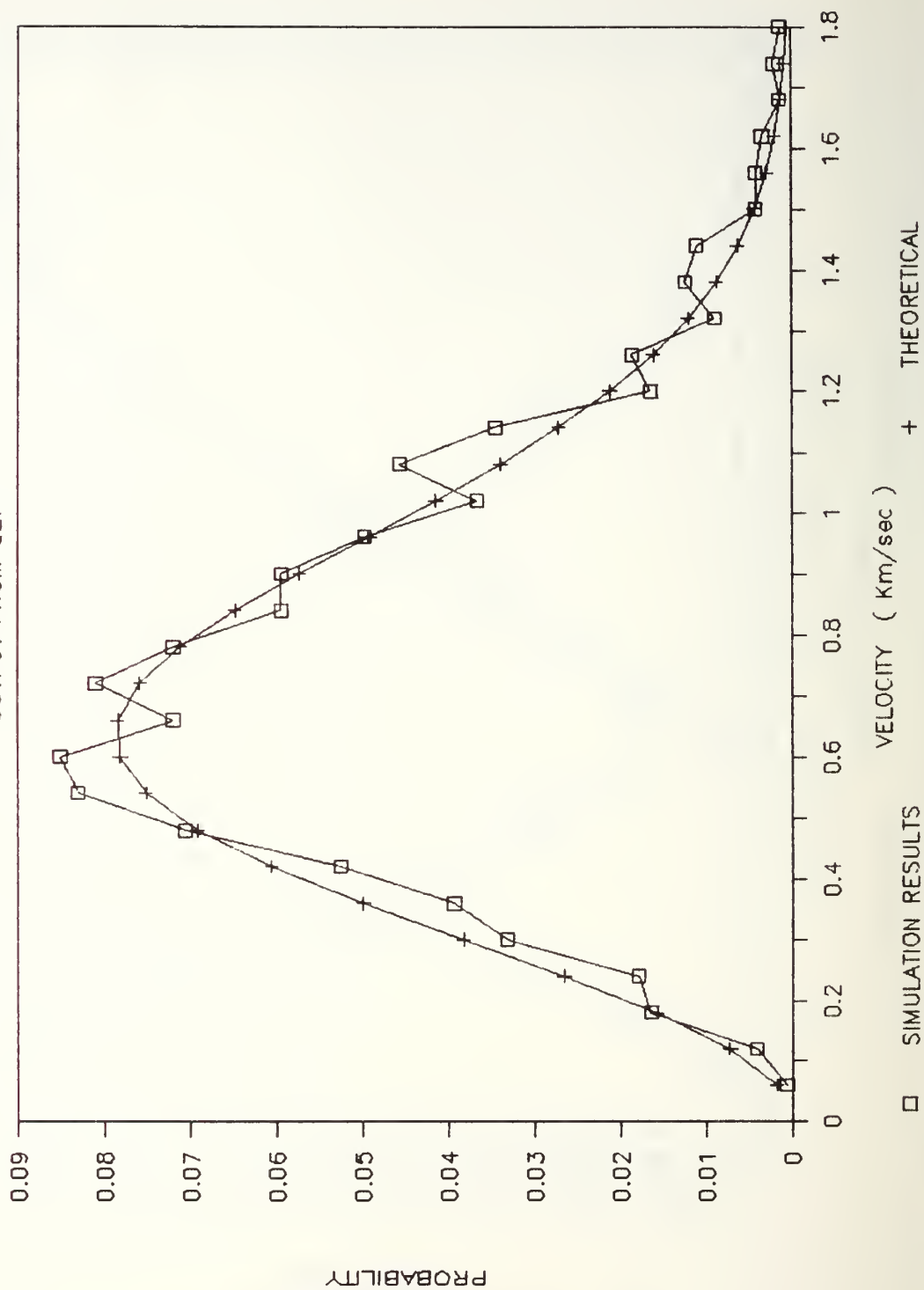
Figure 38. Velocity Distribution, QLV Output.

78
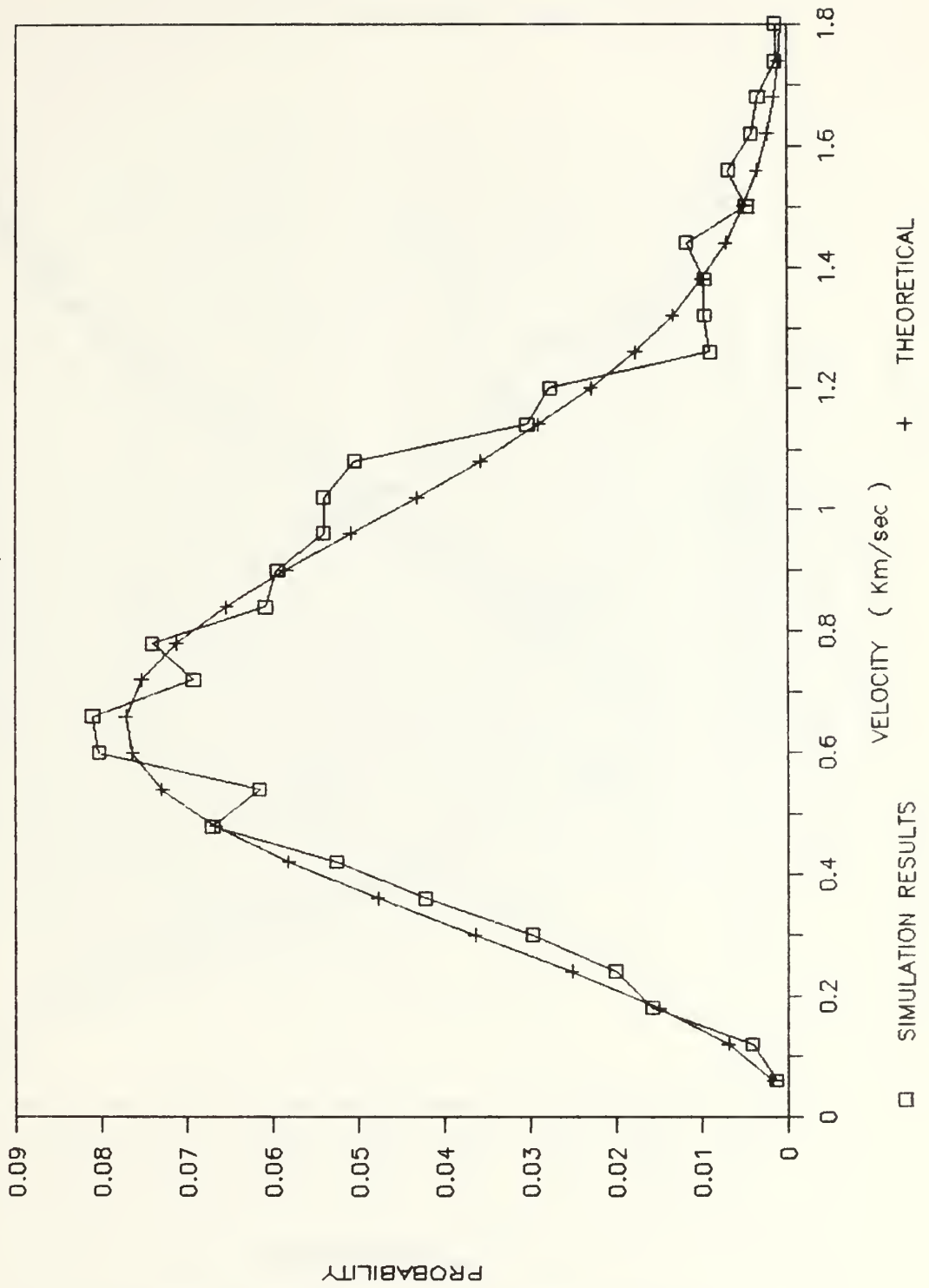
Figure 39. Velocity Distribution, QLVBC Output.

79
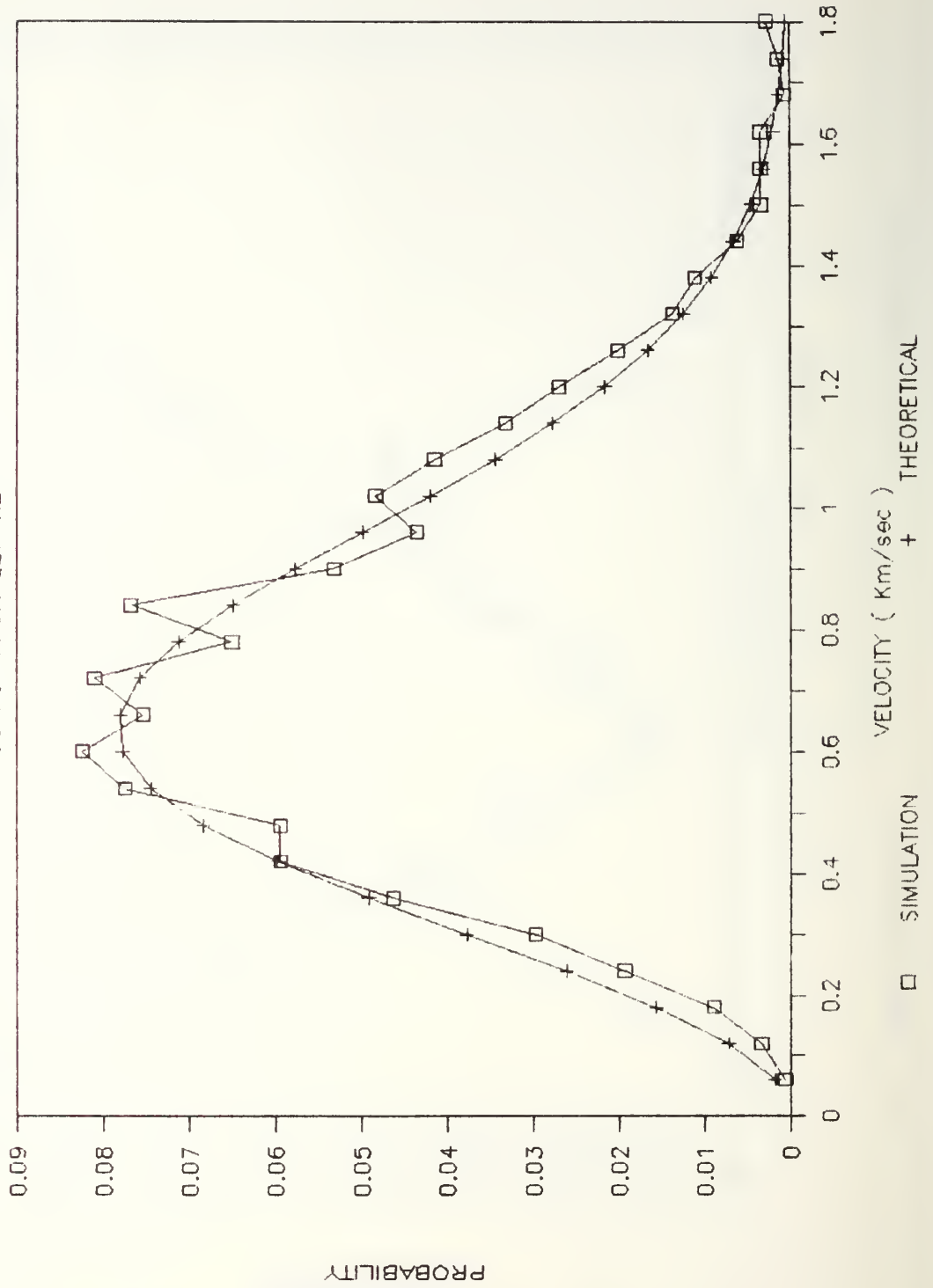
Figure 40. Velocity Distribution, QLV−REV1 Output.

80

Figure 41. Velocity Distribution, QLVBC–REV1 Output.
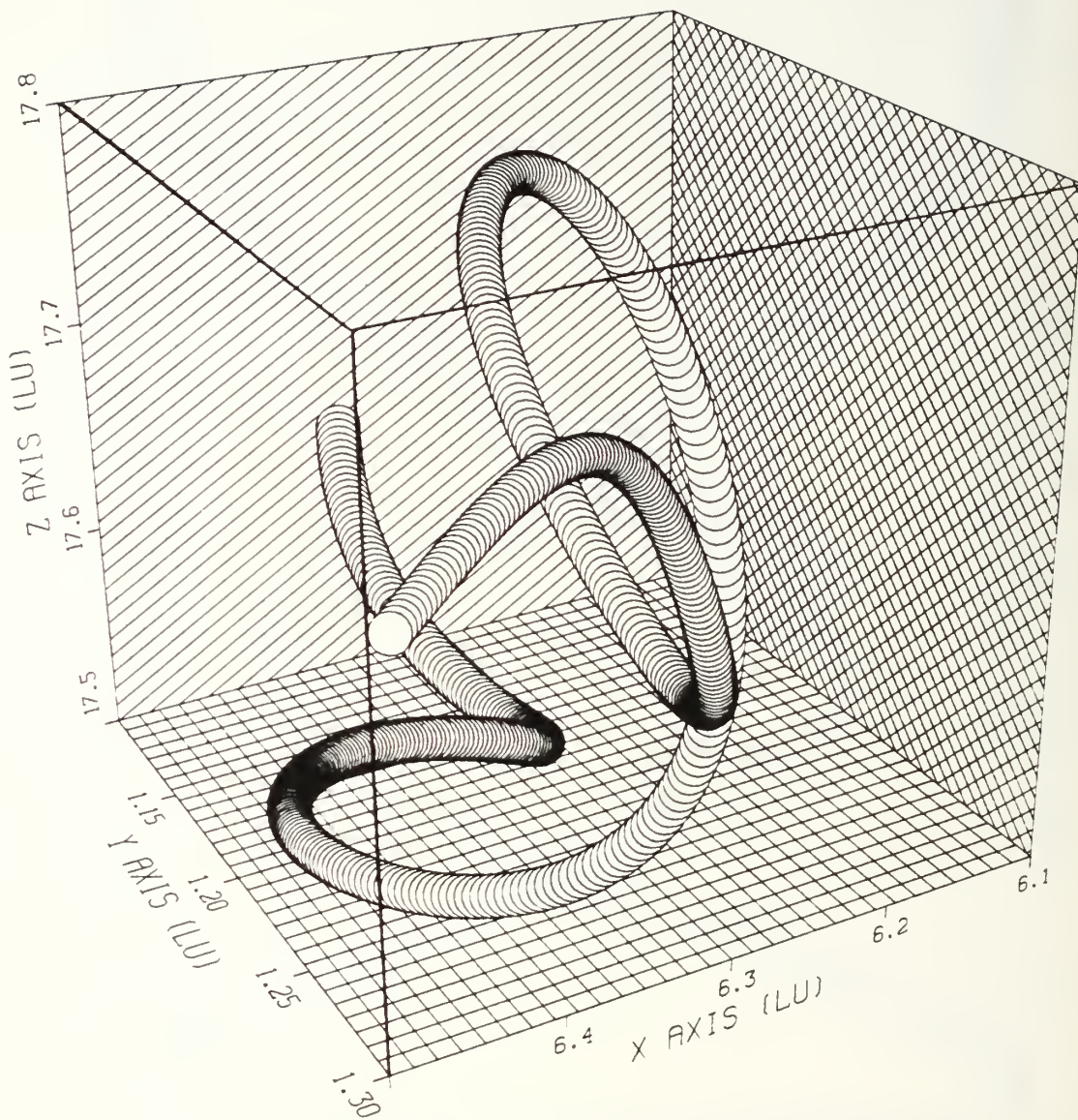
Figure 42. Motion of the Center–Most Atom Under the Influence of its Nearest Neighbors. Output from QLVBC–REV1.

82
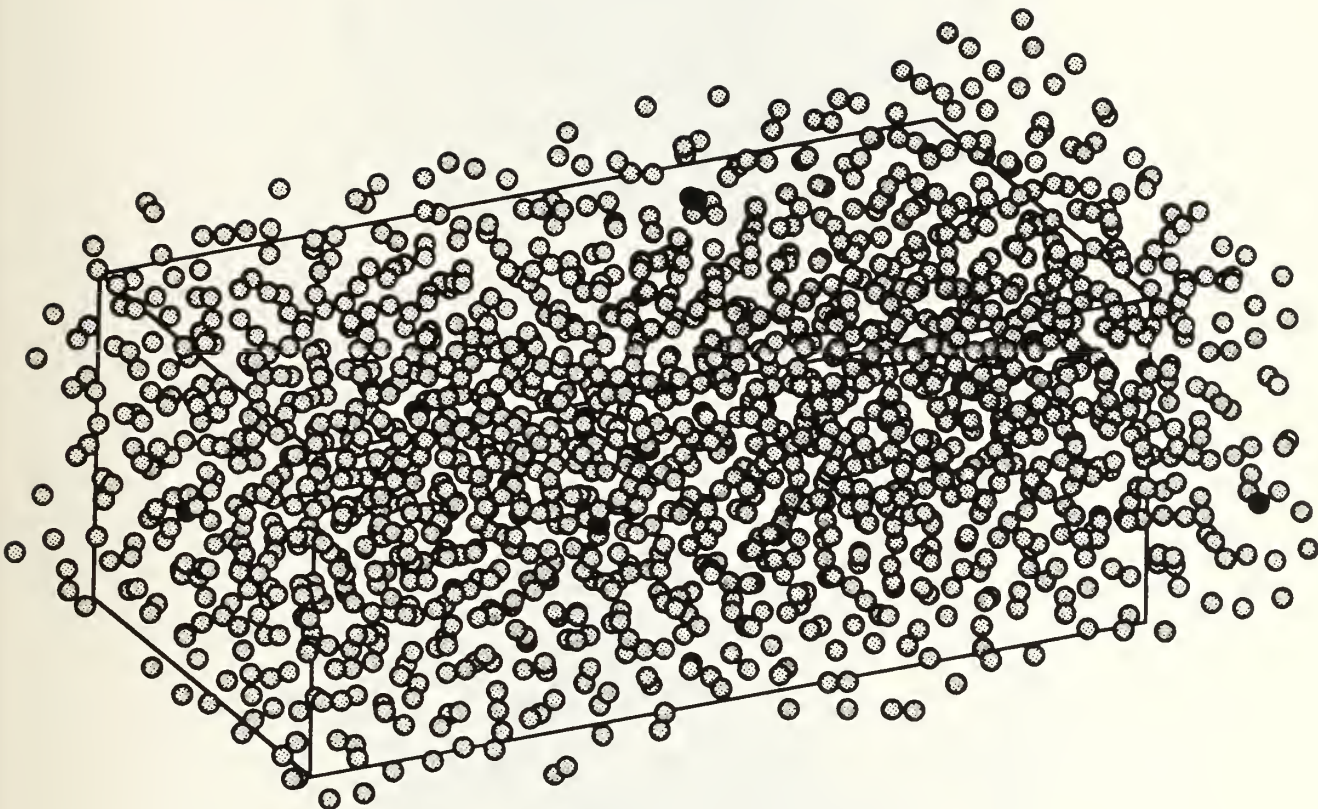
Figure 43. Liquid Copper (Warmed and Equilibrated), QLVBC–REV1
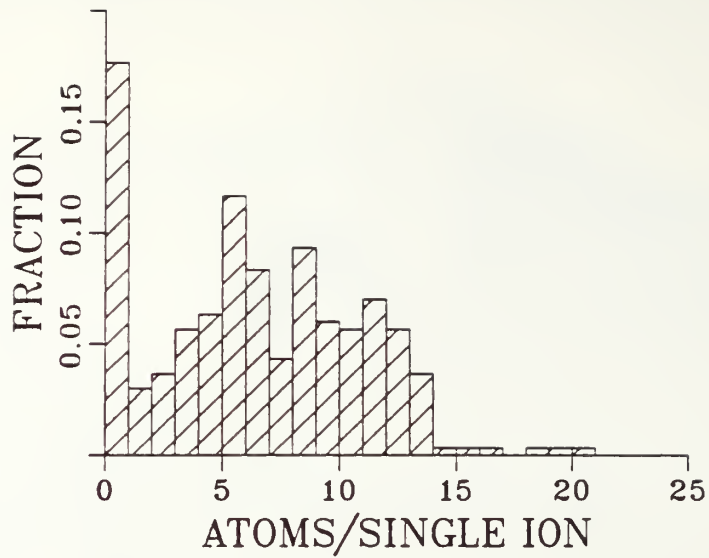
Figure 44. Ejected Atoms per Single Ion for Solid Target, Cu(010) Crystal.
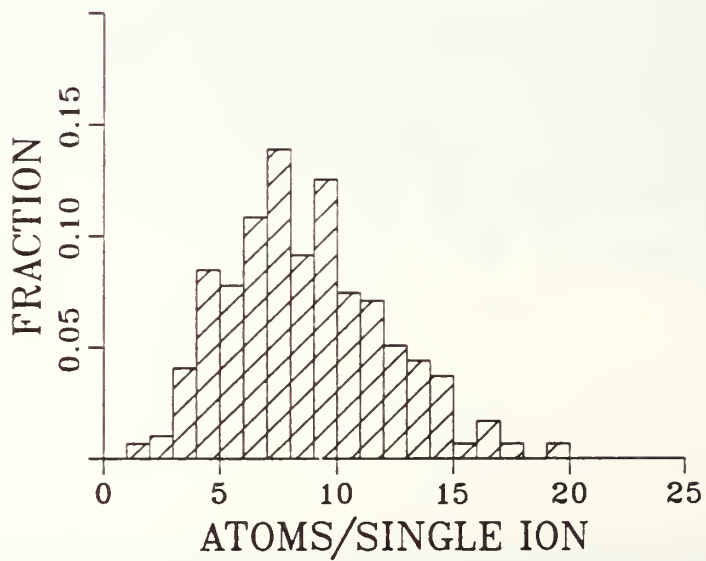
Figure 45. Ejected Atoms per Single Ion for Liquid Target QLVBC−REV1.

84
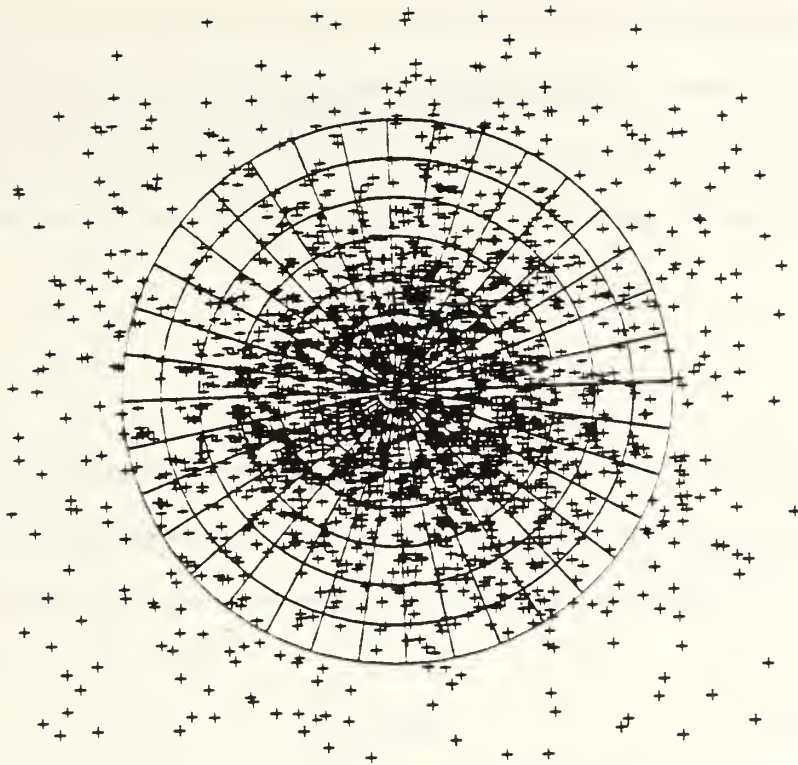
Figure 46. Spot Pattern for Liquid Target QLVBC–REV1.
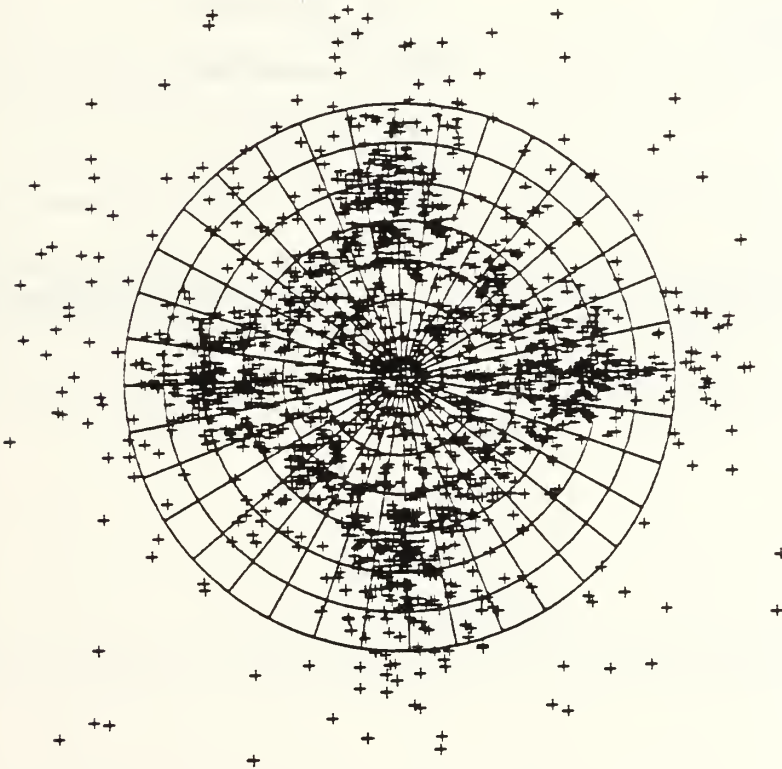
Figure 47. Spot Pattern for Solid Target, Cu(010) Crystal.

85

APPENDIX B – TABLES

TABLE 1	
PHYSICAL DATA FOR COPPER	
Atomic Number (Z)	29
Atomic Weight	63.540 amu
Crystal Type	FCC
Lattice Constant	3.6150 angstroms
R_e	1.8075 angstroms
Melting Point	1083.4 ± 0.2 ^{0}C
Boiling Point	2567 ^{0}C
Density (solid)	8.96 gm/cm^3

Note: Data for Table 1 is derived from reference 59.

TABLE 2		
POTENTIAL FUNCTION PARAMETERS		
Parameter	Cu–Cu	Cu–Ar
A (KeV)	22.564	———
B (A^{-1})	−5.088	———
D_e (eV)	0.431	———
R_e (A)	2.628	———
α (A^{-1})	1.405	———
R_a (LU)	0.83	1.41
R_b (LU)	1.10	1.41
R_c (LU)	2.40	1.41
Z_1 (amu)	29	18
Z_2 (amu)	29	29
K	0.0	0.0920

TABLE 3	
CUBIC SPLINE PARAMETERS	
Parameter	Cu–Cu
C_o	5.876×10^2
C_1	-1.594×10^3
C_2	1.450×10^3
C_3	-4.423×10^2

TABLE 4		
TOTAL ENERGY LOSSES		
Target	Percent Error(%)	Energy Uncertainty(eV)
QLP	0.001	0.04
QLPBC	< 0.001	0.03
QLP–REV1	0.251	6.44
QLPBC–REV1	0.238	6.45
QLV	0.01	0.30
QLVBC	0.01	0.29
QLV–REV1	0.23	6.22
QLVBC–REV1	0.24	4.20

TABLE 5		
DENSITY RESULTS (TARGETS WITH UNRESTRICTED BOUNDARIES)		
	Density (gm/cm³)	
Target	Expected	Result
QLP	7.906	6.646
QLP–REV1	7.906	6.617
QLV	7.806	6.057
QLV–REV1	7.806	7.664

TABLE 6				
KINETIC ENERGY AND TEMPERATURE RESULTS				
	KE (eV)		Temperature (K)	
Target	Expected	Result	Expected	Result
QLP	273.071	265 ± 6	1462.043	1420 ± 32
QLPBC	273.071	273 ± 6	1462.043	1460 ± 32
QLP–REV1	273.071	280 ± 17	1462.043	1520 ± 91
QLPBC–REV1	273.071	290 ± 8	1462.043	1560 ± 43
QLV	296.458	288 ± 9	1587.258	1540 ± 48
QLVBC	296.458	299 ± 12	1587.258	1600 ± 64
QLV–REV1	296.458	315 ± 4	1587.258	1690 ± 21
QLVBC–REV1	296.458	280 ± 4	1587.258	1700 ± 21

Target	1st Peak (LU)	1st Valley (LU)	2nd Peak (LU)	2nd Valley (LU)	3rd Peak (LU)	3rd Valley (LU)
QLP	2.5±.1	——	4.3±.1	——	6.7±.1	——
QLPBC	2.5±.1	——	4.7±.1	——	6.7±.1	——
QLP–REV1	2.4±.1	3.3±.1	4.3±.1	——	6.6±.1	——
QLPBC–REV1	2.4±.1	——	4.4±.1	——	6.6±.1	——
QLV	2.5±.1	——	4.3±.1	——	6.7±.1	——
QLVBC	2.5±.1	——	4.3±.1	——	6.7±.1	——
QLV–REV1	2.4±.1	3.3±.1	4.3±.1	——	6.6±.1	7.7±.1
QLVBC–REV1	2.4±.1	3.3±.1	4.3±.1	5.6±.1	6.5±.1	7.7±.1
NEUTRON DIFF. DATA [ref. 46]	2.5±.1	3.5±.1	4.7±.1	5.6±.1	6.8±.1	7.9±.1

TABLE 7

RADIAL DISTRIBUTIONS, PEAKS AND VALLEYS

TABLE 8		
VELOCITY DIST. χ^2 TESTS TO MAXWELLIAN DIST.		
Target	χ^2	$P_d(\chi^2 \geq \chi^2{}_o)$
QLP	0.9	61.5
QLPBC	1.7	1.6
QLP–REV1	1.7	1.6
QLPBC–REV1	1.9	0.5
QLV	1.5	5.4
QLVBC	1.7	1.6
QLV–REV1	1.5	5.4
QLVBC–REV1	1.5	1.5

TABLE 9					
PERCENT INCREASE IN YIELD OF LIQUID SPUTTERING OVER SOLID SPUTTERING					
Source	Type of Study	Target	Ion	Energy (KeV)	Percent Yield Increase (%)
Ref. 33	experiment	liquid Sn	Argon	0.2 0.4	40 –6
Ref. 34	experiment	liquid Sn	Argon	0.2 0.375	50 15
Ref. 35	experiment	liquid In	Argon	0.107	10
Ref. 43	simulation	liquid Cu	Argon	5.0	60
This Study	simulation	liquid Cu	Argon	1.0	40

LIST OF REFERENCES

1. Plucker, J., "Fortgesetzte Beobachtungen Über die Elektrische Endladung dur Gasverdunnte Raume," Annalen der Physik, v. 103, p. 88, 1858.

2. Grove, W. R., "On the Electro—Chemical Polarity of Gases," Trans. Royal Society of London, v.142, pp.87—102, 1852.

3. Goldstein, E., "The Canal—Ray Group," Verh. Dtsch. Phy. Ges., v. 4, pp. 228—237, 1902.

4. Stark, J., "Volatilisation by Atom Rays," Zeitschrift für Elecktrochem., v. 15, pp. 509—512, 15 July 1909.

5. Thompson, M.W., " The Energy Spectrum of Ejected Atoms During High—Energy Sputtering of Gold," Philosophy Magazine, v. 18, pp. 377—414, August 1969.

6. Bush, V., and Smith C. G., "Control of Gaseous Conduction, " Trans. of Amer. Inst. of Electrical Engineers, v. 41 pp.402—411, 1922.

7. Kingdon, K. H., and Langmuir, I., "The Removal of Thorium from the Surface of Thoriated Tungsten Filament by Positive Ion Bombardment," Physical Review, v. 22, pp.148—160. 1923.

8. Kingdon, K. H., and Langmuir, I., "The Removal of Thorium from the Surface of a Thoriated Tungsten Filament by Bombardment with Positive Ions," Physical Review, v. 20 p. 108, 1922.

9. Blechschmidt, E., "Die Kathodenzerstaubung in Abhangigkeit von den Betriebsbedingungen," Annalen der Physik, v. 81, pp. 99—1042, 1926.

10. Blechschmidt, E., and Von Hipple, A.,"Der Einfluss von Material und Zustand der Kathode auf den Zerstaubungsprozess," Annalen der Physik, v. 86, pp. 1006—1024, 1928.

11. Von Hipple, A., "Zur Theorie der Kathodenzerstaubung," Annalen der Physik, v. 81, pp. 1043—1075, 1926.

12. Von Hipple, A., "Über die Natur und den Ladungszustand der bei Kathodenzerstaubung Emittierten Metallteilchen," Annalen der Physik, v. 80, pp. 672—706, 1926.

13. Lamar, E. S. and Compton, K. T., "A Special Theory of Cathode Sputtering," <u>Science</u>, v. 80,p. 541, 1934.

14 Gutherschultze, A. and Meyer, K., "Kathodenzerstaubung bei sehr Geringen Gasdrucken," <u>Zeitschrift für Physik</u>, v. 62, pp. 607, 1931.

15. Meyer, K.,and Gutherschultze, A., "Kathodenzerstaubung in Quecksilberdampf bei sehr Geringen Drucken," <u>Zeitschrift für Physik</u>, v. 71, pp. 279, 1931.

16. Penning, F. M. and Mobious, J. H. A., "Cathode Sputtering in a Magnetic Field," <u>Koninkl. Ned. Akad. Wetenschop</u>, Proc., V. 43, No.1, pp. 41–56, 1940.

17. Keywell, F., "Radiation Damage Theory of High Vacuum Sputtering," <u>Physical Review</u>, v.97, no. 6, pp. 1611–1615, 15 March 1955.

18. Harrison, D. E., Jr., "Theory of the Sputtering Process," <u>Physics Review</u>, v. 102, pp. 1473–1480, 1956.

19. Wehner, G. K., "Momentum Transfer in Sputtering by Ion Bombardment," <u>Journal of Applied Physics</u>, v. 25, no. 1, pp. 270–271, January 1954.

20. Silsbee,R. H., "Focusing in Collision Problems in Solids," <u>Journal of Applied Physics</u>, v. 28, pp.1246–1250, 1957.

21. Sigmund, P. and Sanders, P., <u>Applications of Ion Beams to Semiconductor Technology</u>, P. Glotin Ed., Editions Ophrys, Grenoble, p. 215., 1967

22. Sigmund, P., <u>Radiation Effects 1</u>, 15(1969).

23. Lindhard, J., Nielsen, V., Scharff, M., and Thompsen, P. V., K. Dan. Vidensk. Selsk. Mat. Fys. Medd. 33, 10 (1963).

24. Sigmund, P., "Theory of Sputtering I. Sputtering Yield of Amorphous and Polycrystalline Targets," <u>Physical Review</u>, 184, pp. 383–415, 1969.

25. Thompson, J. J., <u>Rays of Positive Electricity and Their Applications to Chemical Analysis</u>, Longmans, Green and Co., 1921.

26. Gibson, J. B., et al., "Dynamics of Radiation Damage," <u>Physical Review</u> v. 1028, no. 4, pp. 1229–1253, 15 November 1960.

27. Robinson, M. T. and Oen, O. S., "The Channeling of Energetic Atoms in Crystal Lattices," <u>Applied Physics Letters</u>, v. 2, no. 2, pp. 30–32, 15 January 1963.

28. Harrison, D. E., Jr., et al., "Computer Simulation of Sputtering," <u>Journal of Applied Physics</u>, v. 39, no. 8, pp. 3742–3761, July 1968.

29. Harrison, D. E., Jr., Moore, W.L. and Holocombe, H.T., "Computer Simulation of Sputtering II," Radiation Effects, v. 17, pp. 167–183, 1973.

30. Harrison, D. E., Jr. and Delaplain, C. B., "Computer Simulation of the Sputtering Clusters," Journal of Applied Physics, v. 47, no. 6, pp. 2252–2259, June 1976.

31. Garrison, B. J., Winograd, N. and Harrison, D. E., Jr., "Atomic and Molecular Ejection from Ion Bombarded Reacted Single–Crystal Surfaces: Oxygen on Cu(100)," Physical Review B, v. 18, no. 11, pp. 6000–6010, December 1978.

32. Robinson, M. T. and Torrens, I. M., "Computer Simulation of Atomic–Displacement Cascades in Solid in the Binary Collision Approximation," Physical Review B, v. 9, pp. 5008–5024, 1974.

33. Wehner, G. K., Steward, R. V. and Rosenberg, D., General Mills Report no. 2356, 1962.

34. Krutenat, R. C. and Panzera, C., "Low–Energy Ar^+ Sputtering Yields of Solid and Liquid Tin," Journal of Applied Physics, v. 41, no. 12, November 1970

35. Hurst, B. L. and Cooper C. B., "Low Energy Ar^+ Ion Sputtering of Liquid and Solid Indium," Journal of Applied Physics, v. 53, no. 9, September 1982.

36. Dumke, M. F., Tombrello, T. A., Weller R. A., Housley, R. M. and Cirlin, E. H., "Sputtering of the Gallium–Indium Eutectic Alloy in the Liquid Phase," Technical Report BAP–26, California Institute of Technology, June 1982.

37. Bernal, J. D., Proc. R. Soc., v. A284, pp. 299, 1964

38. Bernal, J. D., "Packing of Spheres," Nature, v. 88, pp. 910, 1960.

39. Finney, J. L., PhD Disertation, University of London, 1968.

40. Verlet, L., "Computer Experiments on Classical Fluids II. Equilibrium Correlation Functions," Physical Review, v. 165, no. 1, January 1968.

41. Miranda , J. M. and Torra, V., "A Molecular Dynamics Study of Liquid Sodium at 373K," Journal of Physics F, v. 13, pp. 281–289, 1983.

42. Lo, D. Y., Tombrello, T. A., Shapiro, M. H.,et al, "Liquid Target Generation Techniques in Molecular Dynamics Studies of Sputtering," Technical Report BB–37, California Institute of Technology, November 1985.

43. Lo, D. Y., Shapiro, M. H., Tombrello, T. A., Garrison, B. J., and Winograd, N., "Simulation Studies of Collision Cascades in Liquid Targets," Technical Report (in press), California Institute of Technology, January 1987.

44. Morgan, W. L., "Dynamical Simulation of Liquid and Solid Metal Self–Sputtering," (in press) Journal of Applied Physics, 6 September 1988.

45. Harrison, D. E., Jr., "Sputter Models – A Synoptic View," Radiation Effects, v. 70, pp. 1,1983.

46. Eder, O. J., Erdpresser, E., Kunsch, B., Stiller, H. and Suda, M., "The Structure Factor of Liquid Copper at 1393K and 1833K," Journal of Physics F: Metal Physics, v. 10, pp. 183–195, 1980.

47. Rice,O. K. Phase Transformations in Solids, John Wiley & Sons, Inc., New York, 1951.

48. Cahill, J. A. and Kirshenbaum, A. D., "The Density of Liquid Copper from Its Melting Point (1356K) to 2500K and an Estimate of Its Critical Constants," Journal of Physics, Chemistry, v. 66, pp.1080, December 1961.

49. Azaroff, L. V.,Elements of X–Ray Crystallography, McGraw–Hill Book Company, New York, 1968.

50. Breuil, M. and Tourand, G., "Determination de la Fonction de Distribution de Paire du Cuivre Liquide par Diffraction de Neutrons," Journal of Physics, Chem. Solids, v. 31, pp. 549–557, 1970.

51. Zei, M. S. and Steffen, B., "X–Ray Diffraction Study of Liquid Gallium and Mercury at Elevated Temperatures," Journal of Physical Chemistry, v. 81, no. 9, 1977

52. Halliday, D. and Resnick, R.,Physics, John Wiley & Sons, New York, 1960.

53. Carter, G. and Colligon, T. S., Ion Bombardment of Solids, American Elsevier Publishing Co., 1968.

54. Sterbenz, H. W., Jr., "A Computer Simulation of Copper Crystal Surface Dynamics," M. S. Thesis, Naval Postgraduate School, Monterey, California, June 1972.

55. Singh, N. and Sharma, P. K., "Debye–Waller Factors of Cubic Metals," Physical Review B, v. 3, no. 4, February 1971.

56. Miller, S. G.,"A Molecular Dynamics Simulation Study of Small Scale Surface Defects Upon Atom Ejection Processes," M. S. Thesis, Naval Postgraduate School, Monterey, California, December 1986.

57. Torrens, I. M.,Interatomic Potentials, Academic, New York, 1972.

58.   Taylor, J. R., An Introduction to Error Analysis, University Science Books, Mill Valley, 1982.

59.   Handbook of Chemistry and Physics, 61st ed., CRC Press, 1980.

INITIAL DISTRIBUTION LIST

No. Copies

1. Defense Technical Information Center   2
    Cameron Station
    Alexandria, Virginia 22304–6145

2. Superintendent   2
    Attn: Library, Code 0142
    Naval Postgraduate School
    Monterey, California 93943–5002

3. Department Chairman, Code 61Sq   2
    Department of Physics
    Naval Postgraduate School
    Monterey, California 93943–5000

4. Roger Smith, Code 61Sm   2
    Department of Physics
    Naval Postgraduate School
    Monterey, California 93943–5000

5. Lieutenant Raul D. Rodriguez   2
    63 NE 11th Way
    Deerfield Beach, Florida 33441